

**Initial gut microbiota and response to antibiotic perturbation
influence *Clostridioides difficile* colonization in mice**

Sarah Tomkovich¹, Joshua M.A. Stough¹, Lucas Bishop¹, Patrick D. Schloss^{1†}

† To whom correspondence should be addressed: pschloss@umich.edu

¹ Department of Microbiology and Immunology, University of Michigan, Ann Arbor, MI 48109

1 Abstract

2 The microbiota plays a key role in determining susceptibility to *Clostridioides difficile* infections
3 (CDIs). However, much of the mechanistic work examining CDIs in mouse models use a single
4 university colony or vendor. We treated mice from 6 different colony sources (2 University of
5 Michigan colonies and 4 vendors) with a single clindamycin dose, followed by *C. difficile* challenge 1
6 day later and measured *C. difficile* colonization levels through 9 days post-infection. The microbiota
7 was profiled via 16S rRNA gene sequencing analysis to examine variation across colony sources
8 and alterations due to clindamycin treatment and *C. difficile* challenge. While all sources of mice
9 were colonized 1-day post-infection, variation in *C. difficile* colonization levels emerged from days
10 3-7 post-infection with 3 sources colonized with *C. difficile* for slightly longer and at higher levels.
11 We identified bacterial taxa with different relative abundances across colony sources throughout the
12 experiment, as well as taxa that were consistently impacted by clindamycin treatment in all sources
13 of mice. We created logistic regression models that successfully classified mice based on whether
14 they cleared *C. difficile* by 7 days post-infection using baseline, post-clindamycin, and post-infection
15 community composition data. After examining the taxa that were most important to the classification
16 models, we identified a subset of key taxa that varied across colony sources (*Bacteroides*,
17 *Deferrribacteraceae*), were altered by clindamycin (*Porphyromonadaceae*, *Ruminococcaceae*), or
18 both (*Enterobacteriaceae*, *Enterococcus*, *Bifidobacteriaceae*, *Coriobacteriaceae*, *Lachnospiraceae*,
19 and *Verrucomicrobiaceae*). These results suggest the response of the initial gut microbiota to
20 clindamycin treatment influences *C. difficile* 630 colonization dynamics.

21 Importance

22 *Clostridioides difficile* is a leading nosocomial infection. Although the microbiota has been
23 established as a key risk factor, there is variation in who becomes asymptotically colonized,
24 develops an infection, or has an infection with adverse outcomes. *C. difficile* infection (CDI) mouse
25 models are widely used to answer a variety of *C. difficile* pathogenesis questions. However, the
26 inter-individual variation between mice is less than what is observed in humans, particularly if just
27 one source of mice is used. In this study, we administered clindamycin to mice from 6 different
28 colony sources and challenged them with *C. difficile*. Interestingly, only a subset of the taxa that

29 vary across sources were associated with how long *C. difficile* was able to colonize. Future studies
30 examining the interplay between the microbiota and *C. difficile* should consider using mice from
31 multiple sources to narrow down the microbes driving the observed phenotypes and reflect human
32 interindividual variation.

33 **Introduction**

34 Antibiotics are a clear risk factor for *Clostridioides difficile* infections (CDIs), but there is variation in
35 who goes on to develop severe or recurrent CDIs after exposure (1, 2). Additionally, asymptomatic
36 colonization, where *C. difficile* is detectable, but symptoms are absent has been documented
37 in infants and adults (3, 4). The intestinal microbiome has been implicated in asymptomatic
38 colonization (5, 6), susceptibility to CDIs (7), and adverse CDI outcomes (9–12).

39 Mouse models of CDIs have been a great tool for understanding *C. difficile* pathogenesis (13). The
40 number of CDI mouse model studies has grown substantially since Chen et al. published their
41 C57BL/6 model in 2008, which disrupted the gut microbiota with antibiotics to enable *C. difficile*
42 colonization and symptoms such as diarrhea and weight loss (14). CDI mouse models have been
43 used to examine translationally relevant questions regarding *C. difficile*, including the role of the
44 microbiota and efficacy of potential therapeutics for treating CDIs (15). However, microbiome
45 variation between lab mice is much less than the variation observed between humans (16, 17).
46 Additionally, studying the contribution of the microbiota to a particular disease phenotype in one set
47 of lab mice after the same perturbation could yield a number of findings of which only a fraction
48 may be driving the phenotype.

49 In the past, our group has attempted to introduce more microbiome variation into the CDI mouse
50 model by using a variety of antibiotic treatments (18–21). An alternative approach to maximize
51 microbiome variation is to use mice from multiple sources (22, 23). Microbiome differences between
52 different mouse vendors have been well documented and shown to influence susceptibility to a
53 variety of diseases (24, 25), including enteric infections (22, 23, 26–30). Additionally, different
54 research groups have observed different CDI outcomes in mice despite using similar models
55 and the microbiome has been proposed as one factor potentially mediating susceptibility (13,
56 18, 21, 31–33). Here we examined how variations in the baseline microbiome and responses to
57 clindamycin treatment in C57BL/6 mice from six different sources influenced susceptibility to *C.*
58 *difficile* colonization and the time needed to clear the infection.

59 **Results**

60 **Clindamycin treatment renders all mice susceptible to *C. difficile* 630 colonization**
61 **regardless of colony source.** To test how the microbiotas of mice from different colony sources
62 impact colonization dynamics after clindamycin exposure, we utilized C57BL/6 mice from 6 different
63 sources: two colonies from the University of Michigan (the Young and Schloss lab colonies), the
64 Jackson Laboratory, Charles River Laboratories, Taconic Biosciences, and Envigo (which was
65 formerly Harlan). These 4 vendors were chosen because they represent commonly used vendors
66 for CDI studies in mice (26, 34–40). After a 13-day acclimation period for the mice ordered from
67 vendors, all mice were treated with 10 mg/kg clindamycin via intraperitoneal injection and one day
68 later challenged with 10^3 *C. difficile* 630 spores (Fig. 1A). Clindamycin was chosen because we
69 have previously demonstrated mice are rendered susceptible, but consistently cleared the CDI
70 within 9 days (21, 41), clindamycin is frequently implicated with human CDIs (42), and is also part of
71 the antibiotic treatment for the frequently cited 2008 CDI mouse model (14). The day after infection,
72 *C. difficile* was detectable in all mice at a similar level (median CFU range: 2.2e+07-1.3e+08; P_{FDR}
73 = 0.15), indicating clindamycin rendered all mice susceptible regardless of colony source (Fig.
74 1B). Interestingly, variation in *C. difficile* CFU levels across sources of mice emerged from days
75 3-7 post-infection (all $P_{FDR} \leq 0.019$; Fig. 1B and Table S1), suggesting mouse colony source is
76 associated with *C. difficile* clearance. We conducted two experiments approximately 3 months
77 apart and while the colonization dynamics were similar across most sources of mice, there was
78 some variation between the 2 experiments, particularly for the Schloss and Envigo mice (Fig.
79 S1A-B, Fig. 1D). Although *C. difficile* 630 causes mild symptoms in mice compared to other *C.*
80 *difficile* strains (43), we also saw that weight change significantly varied across sources of mice with
81 the most weight lost two days post-infection (Fig. 1C, E and Table S2). Interestingly, mice ordered
82 from Jackson, Taconic, and Envigo tended to lose more weight (although there was variation
83 between experiments with Schloss and Envigo mice), have higher *C. difficile* CFU levels and take
84 longer to clear the infection compared to the other sources of mice, which was particularly evident
85 7 days post-infection (Fig. 1B-E), when 57.50 of the mice were still colonized with *C. difficile* (Fig.
86 S1C). By 9 days post-infection the majority of the mice from all sources had cleared *C. difficile* (Fig.
87 S1C) with the exception of 1 Taconic mouse from the first experiment and 2 Envigo mice from the

88 second experiment. Importantly, there was also one Jackson and one Envigo mouse that died
89 between 1- and 3-days post-infection during the second experiment. Thus, clindamycin rendered
90 all mice susceptible to *C. difficile* 630 colonization, regardless of colony source, but variation across
91 sources emerged with 3 out of 6 sources taking longer to clear *C. difficile*.

92 **Bacterial communities consistently vary across mouse colony sources despite antibiotic**
93 **and infection perturbations.** Given the well known variation in mouse microbiomes across
94 vendors and university colonies (25), we hypothesized that the variation in *C. difficile* clearance
95 could be explained by microbiota variation across the 6 sources. We used 16S rRNA gene
96 sequencing to characterize the fecal bacterial communities from the mice over the course of
97 the experiment. Since antibiotics and other risk factors of CDIs are associated with decreased
98 microbiota diversity (44), we first examined alpha diversity measures across the 6 sources of
99 mice. Examining the bacterial communities at baseline, prior to clindamycin treatment there was a
100 significant difference in the number of observed OTUs ($P_{\text{FDR}} = 0.03$), but not Shannon diversity
101 index ($P_{\text{FDR}} = 0.052$) across sources of mice (Fig. 2A-B and Table S3). As expected, clindamycin
102 treatment decreased richness and Shannon diversity across all sources of mice, and communities
103 started to recover 1 day post-infection (Fig. 2C-D). Interestingly, significant differences in diversity
104 metrics across sources ($P_{\text{FDR}} < 0.05$) emerged after both clindamycin and *C. difficile* infection, with
105 Charles River mice having higher richness and Shannon Diversity than most of the other groups
106 (Fig 2C-F and Table S4). While Charles River mice had more diverse microbiotas, Young and
107 Schloss lab mice were also able to clear *C. difficile* faster, suggesting microbiota diversity alone
108 does not explain the observed variation in *C. difficile* colonization across vendors.

109 Next, we compared the bacterial communities from the 6 colonies over the course of the experiment
110 using principal coordinate analysis (PCoA) of the Theta YC distances. Permutational multivariate
111 analysis of variance (PERMANOVA) analysis revealed colony source was the major factor explaining
112 the observed variation across fecal communities ($R^2 = 0.35$, $P = 0.0001$) followed by interactions
113 between cage and day of the experiment (Movie S1 and Table S5). Since, the majority of the
114 perturbations happened over the initial days of the experiment, we decided to focus on the bacterial
115 communities at baseline (day -1), after clindamycin treatment (day 0), and post-infection (day 1). For
116 all 3 timepoints, source and the interaction with cage significantly explained most of the observed

117 community variation (combined $R^2 = 0.90, 0.99, 0.88$, respectively; $P = 0.0001$; Fig. 3 and Table
118 S6). We also compared baseline communities across the 2 experiments, and found experiment
119 and cage significantly explained the observed variation only for the Schloss and Young lab mouse
120 colonies (Fig. S2 and Table S7), although most of the vendors also clustered by experiment,
121 suggesting there was some community variation between the 2 experiments within each vendor.
122 Thus, mouse colony source was the factor that explained the most variation observed in the bacterial
123 communities. Importantly with the exception of the 2 University colonies, the community of each
124 source clustered apart from one another suggesting each community had a unique response to
125 clindamycin treatment and *C. difficile* challenge.

126 Since there was some variation in microbiota communities between experiments at baseline, we
127 next looked at how similar the communities were within the same source and between sources in
128 response to clindamycin treatment and *C. difficile* challenge (Fig. 4) . The baseline communities
129 varied most between experiments for Schloss, Young, and Envigo mice and variation between
130 sources of mice was high (Fig. 4A). Clindamycin treatment reduced variation between experiments
131 within Schloss, Young and Jackson mice and some of the variation between sources diminished
132 (Fig. 4B). Post-infection, the community variation started to increase within sources of mice and
133 variation between sources of mice started to return (Fig. 4C). By using mice from multiple sources
134 we were able to increase the number of microbiota communities we tested with the clindamycin *C.*
135 *difficile* colonization mouse model.

136 After finding differences at the community level, we next identified the taxa that varied across
137 sources of mice over the initial days of the experiment. We examined bacterial relative abundances
138 at the operational taxonomic unit (OTU) and family levels, expecting the number of differences to be
139 reduced at the family level due to the nature of bacterial taxonomy (45). Focusing on the baseline
140 communities first, there were 268 OTUs and 20 families (Table S8-9) with relative abundances that
141 varied across colony sources. Clindamycin treatment reduced the number of taxa with relative
142 abundances that varied across sources to 18 OTUs and 10 families (Table S8-9). After *C. difficile*
143 challenge, there were 44 OTUs and 18 families (Table S8-9) with significantly different relative
144 abundances across sources, as the communities started to recover from antibiotic treatment. In
145 spite of the experimental perturbations that occurred during these 3 timepoints, there were 12

146 OTUs (Fig 5A-C) and 8 families with relative abundances that consistently varied across colony
147 sources (Fig. 5D-F). Importantly, some of the taxa that consistently varied across sources also
148 shifted with clindamycin treatment. For example, *Proteus* increased after clindamycin treatment, but
149 only in Taconic mice. *Enterococcus* was primarily found only in mice purchased from commercial
150 vendors and also increased after clindamycin treatment. In summary, mouse bacterial communities
151 significantly varied according to colony source throughout the course of the experiment and a
152 consistent subset of bacterial taxa remained different across sources regardless of clindamycin
153 and *C. difficile* challenge.

154 **Clindamycin treatment alters a subset of taxa that were found in all colony sources.**
155 Although there were bacteria that consistently varied across colony sources, we also wanted to
156 identify the bacteria that shifted after clindamycin treatment, regardless of colony source. By
157 analyzing all mice that had sequence data from fecal samples collected at baseline and after
158 clindamycin treatment, we identified 153 OTUs and 18 families that were altered after clindamycin
159 treatment (Fig. 6 and Table S10-11). Interestingly, when we compared the list of significant
160 clindamycin impacted bacteria with the bacteria that consistently varied across groups over the
161 initial 3 timepoints of our experiment, we found 3 OTUs (*Lachnospiraceae* (OTU 130), *Lactobacillus*
162 (OTU 6), *Enterococcus* (OTU 23)) and 3 families (*Porphyromonadaceae*, *Enterococcaceae*,
163 *Lachnospiraceae*) overlapped (Fig. 5, Fig. 6C-D). These findings demonstrate that clindamycin has
164 a consistent impact on the fecal bacterial communities of mice from all colony sources and only a
165 subset of the taxa also varied across colony sources.

166 **Source-specific and clindamycin impacted bacteria distinguish *C. difficile* colonization
167 status in mice.** After identifying taxa that varied by colony source, changed after clindamycin
168 treatment, or both, we next wanted to determine which taxa were influencing the variation in *C.*
169 *difficile* colonization at day 7 (Fig. 1D, Fig. S1C). We trained L2-regularized logistic regression
170 models with input bacterial community data from the baseline, post-clindamycin, and post-infection
171 timepoints of the experiment to predict *C. difficile* colonization status on day 7 (Fig. S3A-B). All
172 models were better at predicting *C. difficile* colonization status on day 7 than random chance (all
173 $P \leq 5e-15$; Table S12), however the models trained with OTU level data generally performed
174 better than those trained with family level data with the exception of the models based on

175 the post-infection (day 1) communities (Fig. S3C-D). Interestingly, the model based on the
176 post-clindamycin (day 0) community OTU data performed significantly better than all other models
177 with an AUROC of 0.75 ($P_{FDR} \leq 3.9e-10$ for pairwise comparisons; Table S13). Thus, we were able
178 to use community bacterial relative abundance data alone to differentiate mice that had cleared *C.*
179 *difficile* before day 7 from the mice still colonized with *C. difficile*. Interestingly, the model built with
180 OTU relative abundance data post-clindamycin treatment had the best performance, suggesting
181 how the bacterial community responds to clindamycin treatment has the greatest influence on
182 subsequent *C. difficile* colonization dynamics.

183 Next, to examine the bacteria that were driving each model's performance, we pulled out the top 20
184 taxa that had the highest absolute feature weights in each of the 6 models (Table S14-15). First, we
185 looked at OTUs from the model with the best performance that was based on the post-clindamycin
186 treatment bacterial community data. While most of the 20 OTUs had low relative abundances on day
187 0, *Enterobacteriace*, *Bacteroides* and *Proteus* had high relative abundances in at least one source
188 of mice and significantly varied across sources (Fig. 7A). Next, the top 20 taxa from each model
189 were compared to the list of taxa that varied across colony source (Fig. 5 and Table S8-9) at the
190 same timepoint and the taxa that were altered by clindamycin treatment (Fig. 6 and Table S10-11).
191 We found a subset of OTUs and families that were important to the model and overlapped with
192 bacteria that varied by either source, clindamycin treatment, or both (Fig. S4, S5A-C). Combining
193 the overall results for the 3 OTU models identified 14 OTUs associated with source, 21 OTUs
194 associated with clindamycin treatment, and 6 OTUs associated with both (Fig. 7B). Combining
195 the overall results for the 3 family models identified 18 families associated with source, 14 families
196 associated with clindamycin treatment and 8 families associated with both (Fig. S5D). Several OTUs
197 (*Bacteroides* (OTU 2), *Enterococcus* (OTU 23), *Enterobacteriaceae* (OTU 1), *Porphyromonadaceae*
198 (OTU 7)) and families (*Bacteroidaceae*, *Deferrribacteraceae*, *Enterococcaceae*, *Lachnospiraceae*,
199 *Bifidobacteriaceae*, *Coriobacteriaceae*, *Ruminococcaceae*, *Verrucomicrobiaceae*) appeared across
200 at least 2 models, so we examined how the relative abundances of these key taxa varied over the
201 course of the experiment (Fig. 8 and Fig. S6). Throughout the experiment, there was at least
202 1 timepoint where relative abundances of these taxa significantly varied across sources (Table
203 S16-17). Interestingly, there were no taxa that emerged as consistently enriched or depleted in

204 mice that were colonized past 7 days post-infection with *C. difficile* 630, suggesting multiple bacteria
205 influence the time needed to clear the infection. Together, these results suggest the initial bacterial
206 communities and their responses to clindamycin have a large influence on the time needed to clear
207 *C. difficile*.

208 **Discussion**

209 By examining the *C. difficile* colonization dynamics within mice from 6 different colony sources
210 after perturbing the microbiota with clindamycin treatment, we were able to identify bacterial taxa
211 that were unique to sources throughout the experiment as well as taxa that were universally
212 impacted by clindamycin. We built L2 logistic regression models with baseline, post-clindamycin
213 treatment, and post-infection fecal community data that successfully predicted *C. difficile*
214 colonization status 7 days after infection better than random chance. We identified *Bacteroides*
215 (*OTU 2*), *Enterococcus* (*OTU 23*), *Enterobacteriaceae* (*OTU 1*), *Porphyromonadaceae* (*OTU 7*),
216 *Bacteroidaceae*, *Deferrribacteraceae*, *Enterococcaceae*, *Lachnospiraceae*, *Bifidobacteriaceae*,
217 *Coriobacteriaceae*, *Ruminococcaceae*, *Verrucomicrobiaceae* (Fig. 8, Fig. S6) as candidate bacteria
218 within these communities that were influencing variation in *C. difficile* colonization dynamics since
219 these bacteria were all important in the logistic regression models and varied by colony source,
220 were impacted by clindamycin treatment, or both. Overall, our results demonstrate clindamycin
221 is sufficient to render mice from multiple sources susceptible to CDI and only a subset of the
222 interindividual microbiota variation across mice from different sources was associated with the time
223 needed to clear *C. difficile*.

224 Other groups have taken similar approaches by using mice from multiple colony sources to identify
225 bacteria that either promote colonization resistance or increase susceptibility to enteric infections
226 (22, 23, 26–30). For example, in the context of *Salmonella* infections, *Enterobacteriaceae* and
227 segmented filamentous bacteria have emerged as protective (22, 27). A previous study with *C.*
228 *difficile* identified an endogenous protective *C. difficile* strain LEM1 that bloomed after antibiotic
229 treatment in mice from Jackson or Charles River Laboratories, but not Taconic that protected
230 mice against the more toxigenic *C. difficile* VPI10463 (26). Given that we ordered mice from the
231 same vendors, we checked all mice for endogenous *C. difficile* by plating stool samples that were

232 collected after clindamycin treatment. However, we did not identify any endogenous *C. difficile*
233 strains prior to challenge, suggesting there were no endogenous protective strains in the mice we
234 received and other bacterial taxa mediated the variation in *C. difficile* colonization across sources.
235 Although all mice were susceptible to *C. difficile* colonization, by following colonization over time we
236 found Jackson, Taconic, and Envigo mice remained colonized beyond 7 days post-infection. We
237 identified a subset of bacteria that were important in predicting whether a mouse was still colonized
238 with *C. difficile* 7 days post-infection. These results suggest a subset of the bacterial community is
239 responsible for determining the length of time needed to clear *C. difficile* colonization.

240 In the past variation between different CDI mouse model studies have been attributed to intestinal
241 microbiome differences in mice across different institutional environments. For example, groups
242 using the same clindamycin treatment and C57BL/6 mice had different *C. difficile* outcomes, one
243 having sustained colonization (32), while the other had transient (18). Baseline differences in the
244 microbiota composition have been hypothesized to partially explain the differences in colonization
245 outcomes and overall susceptibility to *C. difficile* after treatment with the same antibiotic (13,
246 31). We have shown that mice from 6 different sources were all susceptible to *C. difficile* 630,
247 suggesting the microbiota influences *C. difficile* clearance more than susceptibility. Fortunately,
248 the bacterial perturbations induced by clindamycin treatment have been well characterized
249 and our findings agree with previous CDI mouse model work demonstrating *Enterococcus* and
250 *Enterobacteriaceae* were associated with *C. difficile* susceptibility and *Porphyromonadaceae*,
251 *Lachnospiraceae*, *Ruminococcaceae*, and *Turicibacter* were associated with resistance (19, 21, 32,
252 33, 41, 46–48). While we have demonstrated that susceptibility is uniform across vendors after
253 clindamycin treatment, there could be different outcomes for either susceptibility or clearance in the
254 case of other antibiotic treatments. The *C. difficile* strain used could also be contributing to the
255 variation in *C. difficile* outcomes seen across different groups (47). We found the time needed
256 to naturally clear *C. difficile* varied across sources of mice implying that at least in the context
257 of the same perturbation, microbiota differences seemed to influence infection outcome more
258 than susceptibility. More importantly, we were able to narrow down from all the variation observed
259 across colony sources to a subset of bacterial taxa that were also important for predicting *C. difficile*
260 colonization status 7 days post-infection. Since all but 3 mice eventually cleared *C. difficile* 630 by 9

261 days post-infection and the model built with the post-clindamycin OTU relative abundance data had
262 the best performance, our results suggest clindamycin treatment had a large role in determining *C.*
263 *difficile* susceptibility and clearance in the mice.

264 Our approach successfully increased the diversity of murine bacterial communities tested in our
265 clindamycin *C. difficile* model. One alternative approach that has been used in some CDI studies
266 (49–54) is to associate mice with human microbiotas. However, a major caveat to this method
267 is the substantial loss of human microbiota community members upon transfer to mice (55, 56).
268 Additionally with the exception of 2 recent studies (49, 50), most of the CDI mouse model studies
269 to date associated mice with just 1 types of human microbiota either from a single donor or a
270 single pool from multiple donors (51–54), which does not aid in the goal of figuring out how a
271 variety of unique microbiotas influence susceptibility to CDIs and adverse outcomes. Encouragingly,
272 decreased *Bifidobacterium*, *Porphyromonas*, *Ruminococcaceae* and *Lachnospiraceae* and
273 increased *Enterobacteriaceae*, *Enterococcus*, *Lactobacillus*, and *Proteus* have all been associated
274 with human CDIs (7) and were well represented in our study, suggesting most of the mouse
275 sources are suitable for gaining insights into microbiota associated factors influencing *C. difficile*
276 colonization and infections in humans. An important exception was *Enterococcus*, which was
277 primarily absent from the mice from University of Michigan colonies and *Proteus*, which was only
278 found in Taconic mice. Importantly, the fact that some CDI associated bacteria were only found in a
279 subset of mice has important implications for future CDI mouse model studies.

280 There are several limitations to our work. The microbiome is composed of viruses, fungi, and
281 parasites in addition to bacteria, and these non-bacterial members can also vary across mouse
282 vendors (57, 58). While our study focused solely on the bacterial portion, viruses and fungi have
283 also begun to be implicated in the context of CDIs or FMT treatments for recurrent CDIs (35, 59–62).
284 Beyond community composition, the metabolic function of the microbiota also has a CDI signature
285 (20, 48, 63, 64) and can vary across mice from different sources (65). For example, microbial
286 metabolites, particularly secondary bile acids and butyrate production, have been implicated as
287 important contributors to *C. difficile* resistance (33, 47). Although, we only looked at composition,
288 *Ruminococcaceae* and *Lachnospiraceae* both emerged as important taxa for classifying day 7 *C.*
289 *difficile* colonization status and metagenomes from these bacteria have been shown to contain

290 the bile acid-inducible gene cluster necessary for secondary bile acid formation and ability to
291 produce butyrate (52, 66). Interestingly, butyrate has previously been shown to vary across vendors
292 and mediates resistance to *Citrobacter rodentium* infection, a model of enterohemorrhagic and
293 enteropathogenic *Escherichia coli* infections (23). Evidence for immunological toning differences in
294 IgA and Th17 cells across mice from different vendors have also been documented and (67, 68) may
295 also influence response to CDI, particularly in the context of severe CDIs (69, 70). The outcome
296 after *C. difficile* exposure depends on a multitude of factors, including age, diet, and immunity; all of
297 which are also influenced by the microbiota. We have demonstrated that the ways different baseline
298 microbiotas from different mouse colony sources respond to clindamycin treatment influences the
299 length of time mice remained colonized with *C. difficile* 630. For those interested in dissecting the
300 contribution of the microbiome to *C. difficile* pathogenesis and treatments, using multiple sources
301 of mice may yield more insights than a single model alone. Furthermore, for studies wanting to
302 examine the interplay between a particular bacterial taxon such as *Enterococcus* and *C. difficile*,
303 these results could serve as a resource for selecting which mice to order to address the question.

304 **Acknowledgements**

305 This work was supported by the National Institutes of Health (U01AI124255). ST was supported by
306 the Michigan Institute for Clinical and Health Research Postdoctoral Translation Scholars Program
307 (UL1TR002240). We thank members of the Schloss lab for feedback on planning the experiments
308 and data presentation, as well as code tutorials and feedback through Code club. In particular, we
309 want to thank Begüm Topçuoğlu for help with implementing L2 logistic regression models using
310 her pipeline, Ana Taylor for help with some media preparation and sample collection, and Nicholas
311 Lesniak for his critical feedback on the manuscript. We also thank members of Vincent Young's
312 lab, particularly Kimberly Vendrov, for guidance with the *C. difficile* infection mouse model and
313 donating the mice. We also want to thank the Unit for Laboratory Animal Medicine at the University
314 of Michigan for maintaining our mouse colony and providing the institutional support for our mouse
315 experiments. Finally, we thank Kwi Kim, Austin Campbell, and Kimberly Vendrov for their help in
316 maintaining the Schloss lab's anaerobic chamber.

317 **Materials and Methods**

318 **(i) Animals.** All experiments were approved by the University of Michigan Animal Care and Use
319 Committee (IACUC) under protocol number PRO00006983. Female C57BL/7 mice were obtained
320 from 6 different colony sources: The Jackson Laboratory, Charles River Laboratories, Taconic
321 Biosciences, Envigo, and two colonies at the University of Michigan (the Schloss lab colony and
322 the Young lab colony). The Young lab colony was originally established with mice purchased from
323 Jackson, and the Schloss lab colony was later founded with mice donated from the Young lab. The
324 4 groups of mice purchased from vendors were allowed to acclimate to the University of Michigan
325 mouse facility for 13 days prior to starting the experiment. At least 4 female mice (age 5-10 weeks)
326 were obtained per source and mice from the same source were primarily housed at a density of 2
327 mice per cage. The experiment was repeated once, approximately 3 months after the start of the
328 first experiment.

329 **(ii) Antibiotic treatment.** After the 13-day acclimation period and 1 day prior to challenge (Fig.
330 1A), all mice received 10 mg/kg clindamycin (filter sterilized through a 0.22 micron syringe filter
331 prior to administration) via intraperitoneal injection.

332 **(iii) *C. difficile* infection model.** Mice were challenged with 10^3 spores of *C. difficile* strain 630
333 via oral gavage post-infection 1 day after clindamycin treatment as described previously (21). Mice
334 weights and stool samples were taken daily through 9 days post-challenge. Collected stool was
335 split for *C. difficile* CFU quantification and 16S rRNA sequencing analysis. *C. difficile* quantification
336 stool samples were transferred to the anaerobic chamber, serially diluted in PBS, plated on
337 taurocholate-cycloserine-cefoxitin-fructose agar (TCCFA) plates, and counted after 24 hours of
338 incubation at 37°C under anaerobic conditions. A sample from the day 0 timepoint (post-clindamycin
339 and prior to *C. difficile* challenge) was also plated on TCCFA to ensure mice were not already
340 colonized with *C. difficile* prior to infection. There were 3 deaths recorded over the course of the
341 experiment, 1 Taconic mouse died prior to *C. difficile* challenge and 1 Jackson and 1 Envigo mouse
342 died between 1- and 3-days post-infection. Mice were categorized as cleared when no *C. difficile*
343 was detected in the first serial dilution (limit of detection: 100 CFU). Stool samples for 16S rRNA
344 sequencing were snap frozen in liquid nitrogen and stored at -80°C until DNA extraction.

345 **(iv) 16S rRNA sequencing.** DNA was extracted from -80 °C stored stool samples using the DNeasy
346 Powersoil HTP 96 kit (Qiagen) and an EpMotion 5075 automated pipetting system (Eppendorf).
347 The V4 region was amplified for 16S rRNA with the AccuPrime Pfx DNA polymerase (Thermo
348 Fisher Scientific) using custom barcoded primers, as previously described (71). The ZymoBIOMICS
349 microbial community DNA standards was used as a mock community control (72) and water was
350 used as a negative control per 96-well extraction plate. The PCR amplicons were cleaned up
351 and normalized with the SequalPrep normalization plate kit (Thermo Fisher Scientific). Amplicons
352 were pooled and quantified with the KAPA library quantification kit (KAPA biosystems), prior to
353 sequencing using the MiSeq system (Illumina).

354 **(v) 16S rRNA gene sequence analysis.** mothur (v. 1.43) was used to process all sequences
355 (73) with a previously published protocol (71). Reads were combined and aligned with the SILVA
356 reference database (74). Chimeras were removed with the VSEARCH algorithm and taxonomic
357 assignment was completed with a modified version (v16) of the Ribosomal Database Project
358 reference database (v11.5) (75) with an 80% cutoff. Operational taxonomic units (OTUs) were
359 assigned with a 97% similarity threshold using the opticlus algorithm (76). To account for uneven
360 sequencing across samples, samples were rarefied to 5,437 sequences 1,000 times for alpha and
361 beta diversity analyses. PCoAs were generated based on Theta YC distances. Permutational
362 multivariate analysis of variance (PERMANOVA) was performed on mothur-generated Theta YC
363 distance matrices with the adonis function in the vegan package (77) in R (78).

364 **(vi) Classification model training and evaluation.** Models were generated based on mice that
365 were categorized as either cleared or colonized 7 days post-infection and had sequencing data
366 from the baseline (day -1), post-clindamycin (day 0), and post-infection (day 1) timepoints of the
367 experiment. Input bacterial community relative abundance data at either the OTU or family level from
368 the baseline, post-clindamycin, and post-infection timepoints was used to generate 6 classification
369 models that predicted *C. difficile* colonization status 7 days post-infection. The L2-regularized
370 logistic regression models were trained and tested using the caret package (79) in R as previously
371 described (80) with the exception that we used 60% training and 40% testing data splits for the
372 cross-validation of the training data to select the best cost hyperparameter and the testing of
373 the held out test data to measure model performance. The modified training/testing ratio was

374 selected to accommodate the small number of samples in the dataset. Code was modified from
375 https://github.com/SchlossLab/ML_pipeline_microbiome to update the classification outcomes and
376 change the data split ratios. The modified repository to regenerate this analysis is available at
377 https://github.com/tomkosev/ML_pipeline_microbiome.

378 **(vii) Statistical analysis.** All statistical tests were performed in R (v 3.5.2) (78). The Kruskal-Wallis
379 test was used to analyze differences in *C. difficile* CFU, mouse weight change, and alpha diversity
380 across vendors with a Benjamini-Hochberg correction for testing multiple timepoints, followed by
381 pairwise Wilcoxon comparisons with Benjamini-Hochberg correction. For taxonomic analysis and
382 generation of logistic regression model input data, *C. difficile* (OTU 20) was removed. Bacterial
383 relative abundances that varied across sources at the OTU and family taxonomic levels were
384 identified with the Kruskal-Wallis test with Benjamini-Hochberg correction for testing all identified
385 taxa at each level, followed by pairwise Wilcoxon comparisons with Benjamini-Hochberg correction.
386 Taxa impacted by clindamycin treatment were identified using the Wilcoxon signed rank test with
387 matched pairs of mice samples for day -1 and day 0. To determine whether classification models had
388 better performance (test AUROCs) than random chance (0.5), we used the one-sample Wilcoxon
389 signed rank test. To examine whether there was an overall difference in predictive performance
390 across the 6 classification models we used the Kruskal-Wallis test followed by pairwise Wilcoxon
391 comparisons with Benjamini-Hochberg correction for multiple hypothesis testing. The tidyverse
392 package was used to wrangle and graph data (v 1.3.0) (81).

393 **(viii) Code availability.** Code for all data analysis and generating this manuscript is available at
394 https://github.com/SchlossLab/Tomkovich_vendor_difs_XXXX_2020.

395 **(ix) Data availability.** The 16S rRNA sequencing data have been deposited in the National Center
396 for Biotechnology Information Sequence Read Archive (BioProject Accession no. PRJNA608529).

397 **References**

- 398 1. Teng C, Reveles KR, Obodozie-Ofoegbu OO, Frei CR. 2019. *Clostridium difficile* infection
399 risk with important antibiotic classes: An analysis of the FDA adverse event reporting system.
400 International Journal of Medical Sciences 16:630–635.
- 401 2. Kelly C. 2012. Can we identify patients at high risk of recurrent *Clostridium difficile* infection?
402 Clinical Microbiology and Infection 18:21–27.
- 403 3. Zacharioudakis IM, Zervou FN, Pliakos EE, Ziakas PD, Mylonakis E. 2015. Colonization with
404 toxinogenic *C. difficile* upon hospital admission, and risk of infection: A systematic review and
405 meta-analysis. American Journal of Gastroenterology 110:381–390.
- 406 4. Crobach MJT, Vernon JJ, Loo VG, Kong LY, Péchiné S, Wilcox MH, Kuijper EJ. 2018.
407 Understanding *Clostridium difficile* colonization. Clinical Microbiology Reviews 31.
- 408 5. Zhang L, Dong D, Jiang C, Li Z, Wang X, Peng Y. 2015. Insight into alteration of gut microbiota
409 in *Clostridium difficile* infection and asymptomatic *c. difficile* colonization. Anaerobe 34:1–7.
- 410 6. VanInsberghe D, Elsherbini JA, Varian B, Poutahidis T, Erdman S, Polz MF. 2020. Diarrhoeal
411 events can trigger long-term *Clostridium difficile* colonization with recurrent blooms. Nature
412 Microbiology 5:642–650.
- 413 7. Mancabelli L, Milani C, Lugli GA, Turroni F, Cocconi D, Sinderen D van, Ventura M. 2017.
414 Identification of universal gut microbial biomarkers of common human intestinal diseases by
415 meta-analysis. FEMS Microbiology Ecology 93.
- 416 8. Duvallet C, Gibbons SM, Gurry T, Irizarry RA, Alm EJ. 2017. Meta-analysis of gut microbiome
417 studies identifies disease-specific and shared responses. Nature Communications 8.
- 418 9. Seekatz AM, Rao K, Santhosh K, Young VB. 2016. Dynamics of the fecal microbiome in patients
419 with recurrent and nonrecurrent *Clostridium difficile* infection. Genome Medicine 8.
- 420 10. Khanna S, Montassier E, Schmidt B, Patel R, Knights D, Pardi DS, Kashyap PC. 2016. Gut
421 microbiome predictors of treatment response and recurrence in primary *Clostridium difficile* infection.

- 422 Alimentary Pharmacology & Therapeutics 44:715–727.
- 423 11. Pakpour S, Bhanvadia A, Zhu R, Amarnani A, Gibbons SM, Gurry T, Alm EJ, Martello LA. 2017.
424 Identifying predictive features of *Clostridium difficile* infection recurrence before, during, and after
425 primary antibiotic treatment. Microbiome 5.
- 426 12. Lee AA, Rao K, Limsrivilai J, Gilliland M, Malamet B, Briggs E, Young VB, Higgins PDR. 2020.
427 Temporal gut microbial changes predict recurrent *Clostridioides difficile* infection in patients with
428 and without ulcerative colitis. Inflammatory Bowel Diseases.
- 429 13. Hutton ML, Mackin KE, Chakravorty A, Lyras D. 2014. Small animal models for the study of
430 *Clostridium difficile* disease pathogenesis. FEMS Microbiology Letters 352:140–149.
- 431 14. Chen X, Katchar K, Goldsmith JD, Nanthakumar N, Cheknis A, Gerding DN, Kelly CP. 2008. A
432 mouse model of *Clostridium difficile*-associated disease. Gastroenterology 135:1984–1992.
- 433 15. Best EL, Freeman J, Wilcox MH. 2012. Models for the study of *Clostridium difficile* infection.
434 Gut Microbes 3:145–167.
- 435 16. Baxter NT, Wan JJ, Schubert AM, Jenior ML, Myers P, Schloss PD. 2014. Intra- and
436 interindividual variations mask interspecies variation in the microbiota of sympatric peromyscus
437 populations. Applied and Environmental Microbiology 81:396–404.
- 438 17. Nagpal R, Wang S, Woods LCS, Seshie O, Chung ST, Shively CA, Register TC, Craft S,
439 McClain DA, Yadav H. 2018. Comparative microbiome signatures and short-chain fatty acids in
440 mouse, rat, non-human primate, and human feces. Frontiers in Microbiology 9.
- 441 18. Reeves AE, Theriot CM, Bergin IL, Huffnagle GB, Schloss PD, Young VB. 2011. The interplay
442 between microbiome dynamics and pathogen dynamics in a murine model of *Clostridium difficile*
443 infection 2:145–158.
- 444 19. Schubert AM, Sinani H, Schloss PD. 2015. Antibiotic-induced alterations of the murine gut
445 microbiota and subsequent effects on colonization resistance against *Clostridium difficile*. mBio 6.
- 446 20. Jenior ML, Leslie JL, Young VB, Schloss PD. 2017. *Clostridium difficile* colonizes alternative

- 447 nutrient niches during infection across distinct murine gut microbiomes. *mSystems* 2.
- 448 21. Jenior ML, Leslie JL, Young VB, Schloss PD. 2018. *Clostridium difficile* alters the structure and
449 metabolism of distinct cecal microbiomes during initial infection to promote sustained colonization.
450 *mSphere* 3.
- 451 22. Velazquez EM, Nguyen H, Heasley KT, Saechao CH, Gil LM, Rogers AWL, Miller BM, Rolston
452 MR, Lopez CA, Litvak Y, Liou MJ, Faber F, Bronner DN, Tiffany CR, Byndloss MX, Byndloss
453 AJ, Bäumler AJ. 2019. Endogenous Enterobacteriaceae underlie variation in susceptibility to
454 *Salmonella* infection. *Nature Microbiology* 4:1057–1064.
- 455 23. Osbelt L, Thiemann S, Smit N, Lesker TR, Schröter M, Gálvez EJC, Schmidt-Hohagen K, Pils
456 MC, Mühlen S, Dersch P, Hiller K, Schlüter D, Neumann-Schaal M, Strowig T. 2020. Variations in
457 microbiota composition of laboratory mice influence *Citrobacter rodentium* infection via variable
458 short-chain fatty acid production. *PLOS Pathogens* 16:e1008448.
- 459 24. Stough JMA, Dearth SP, Denny JE, LeCleir GR, Schmidt NW, Campagna SR, Wilhelm SW.
460 2016. Functional characteristics of the gut microbiome in C57BL/6 mice differentially susceptible to
461 *Plasmodium yoelii*. *Frontiers in Microbiology* 7.
- 462 25. Alegre M-L. 2019. Mouse microbiomes: Overlooked culprits of experimental variability. *Genome
463 Biology* 20.
- 464 26. Etienne-Mesmin L, Chassaing B, Adekunle O, Mattei LM, Bushman FD, Gewirtz AT. 2017.
465 Toxin-positive *Clostridium difficile* latently infect mouse colonies and protect against highly
466 pathogenic *C. difficile*. *Gut* 67:860–871.
- 467 27. Lai NY, Musser MA, Pinho-Ribeiro FA, Baral P, Jacobson A, Ma P, Potts DE, Chen Z, Paik D,
468 Soualhi S, Yan Y, Misra A, Goldstein K, Lagomarsino VN, Nordstrom A, Sivanathan KN, Wallrapp A,
469 Kuchroo VK, Nowarski R, Starnbach MN, Shi H, Surana NK, An D, Wu C, Huh JR, Rao M, Chiu IM.
470 2020. Gut-innervating nociceptor neurons regulate peyer's patch microfold cells and SFB levels to
471 mediate *Salmonella* host defense. *Cell* 180:33–49.e22.
- 472 28. Thiemann S, Smit N, Roy U, Lesker TR, Gálvez EJ, Helmecke J, Basic M, Bleich A, Goodman

- 473 AL, Kalinke U, Flavell RA, Erhardt M, Strowig T. 2017. Enhancement of IFNgamma production by
474 distinct commensals ameliorates *Salmonella*-induced disease. *Cell Host & Microbe* 21:682–694.e5.
- 475 29. Rolig AS, Cech C, Ahler E, Carter JE, Ottemann KM. 2013. The degree of *Helicobacter*
476 *pylori*-triggered inflammation is manipulated by preinfection host microbiota. *Infection and Immunity*
477 81:1382–1389.
- 478 30. Ge Z, Sheh A, Feng Y, Muthupalani S, Ge L, Wang C, Kurnick S, Mannion A, Whary MT, Fox
479 JG. 2018. *Helicobacter pylori*-infected C57BL/6 mice with different gastrointestinal microbiota have
480 contrasting gastric pathology, microbial and host immune responses. *Scientific Reports* 8.
- 481 31. Lawley TD, Young VB. 2013. Murine models to study *Clostridium difficile* infection and
482 transmission. *Anaerobe* 24:94–97.
- 483 32. Buffie CG, Jarchum I, Equinda M, Lipuma L, Gobourne A, Viale A, Ubeda C, Xavier J, Pamer
484 EG. 2011. Profound alterations of intestinal microbiota following a single dose of clindamycin results
485 in sustained susceptibility to *Clostridium difficile*-induced colitis. *Infection and Immunity* 80:62–73.
- 486 33. Buffie CG, Bucci V, Stein RR, McKenney PT, Ling L, Gobourne A, No D, Liu H, Kinnebrew
487 M, Viale A, Littmann E, Brink MRM van den, Jenq RR, Taur Y, Sander C, Cross JR, Toussaint
488 NC, Xavier JB, Pamer EG. 2014. Precision microbiome reconstitution restores bile acid mediated
489 resistance to *Clostridium difficile*. *Nature* 517:205–208.
- 490 34. Spinler JK, Brown A, Ross CL, Boonma P, Conner ME, Savidge TC. 2016. Administration of
491 probiotic kefir to mice with *Clostridium difficile* infection exacerbates disease. *Anaerobe* 40:54–57.
- 492 35. Markey L, Shaban L, Green ER, Lemon KP, Mecsas J, Kumamoto CA. 2018. Pre-colonization
493 with the commensal fungus candida albicans reduces murine susceptibility to *Clostridium difficile*
494 infection. *Gut Microbes* 1–13.
- 495 36. McKee RW, Aleksanyan N, Garrett EM, Tamayo R. 2018. Type IV pili promote *Clostridium*
496 *difficile* adherence and persistence in a mouse model of infection. *Infection and Immunity* 86.
- 497 37. Yamaguchi T, Konishi H, Aoki K, Ishii Y, Chono K, Tateda K. 2020. The gut microbiome diversity

- 498 of *Clostridioides difficile*-inoculated mice treated with vancomycin and fidaxomicin. Journal of
499 Infection and Chemotherapy 26:483–491.
- 500 38. Stroke IL, Letourneau JJ, Miller TE, Xu Y, Pechik I, Savoly DR, Ma L, Sturzenbecker LJ,
501 Sabalski J, Stein PD, Webb ML, Hilbert DW. 2018. Treatment of *Clostridium difficile* infection
502 with a small-molecule inhibitor of toxin UDP-glucose hydrolysis activity. Antimicrobial Agents and
503 Chemotherapy 62.
- 504 39. Quigley L, Coakley M, Alemayehu D, Rea MC, Casey PG, O'Sullivan, Murphy E, Kiely B, Cotter
505 PD, Hill C, Ross RP. 2019. *Lactobacillus gasseri* APC 678 reduces shedding of the pathogen
506 *Clostridium difficile* in a murine model. Frontiers in Microbiology 10.
- 507 40. Mullish BH, McDonald JAK, Pechlivanis A, Allegretti JR, Kao D, Barker GF, Kapila D, Petrof
508 EO, Joyce SA, Gahan CGM, Glegola-Madejska I, Williams HRT, Holmes E, Clarke TB, Thursz
509 MR, Marchesi JR. 2019. Microbial bile salt hydrolases mediate the efficacy of faecal microbiota
510 transplant in the treatment of recurrent *Clostridioides difficile* infection. Gut 68:1791–1800.
- 511 41. Tomkovich S, Lesniak NA, Li Y, Bishop L, Fitzgerald MJ, Schloss PD. 2019. The proton
512 pump inhibitor omeprazole does not promote *Clostridioides difficile* colonization in a murine model.
513 mSphere 4.
- 514 42. Guh AY, Kutty PK. 2018. *Clostridioides difficile* infection 169:ITC49.
- 515 43. Theriot CM, Koumpouras CC, Carlson PE, Bergin II, Aronoff DM, Young VB. 2011.
516 Cefoperazone-treated mice as an experimental platform to assess differential virulence of
517 *Clostridium difficile* strains. Gut Microbes 2:326–334.
- 518 44. Ross CL, Spinler JK, Savidge TC. 2016. Structural and functional changes within the gut
519 microbiota and susceptibility to *Clostridium difficile* infection. Anaerobe 41:37–43.
- 520 45. Nguyen TLA, Vieira-Silva S, Liston A, Raes J. 2015. How informative is the mouse for human
521 gut microbiota research? Disease Models & Mechanisms 8:1–16.
- 522 46. Lawley TD, Clare S, Walker AW, Goulding D, Stabler RA, Croucher N, Mastroeni P, Scott P,

- 523 Raisen C, Mottram L, Fairweather NF, Wren BW, Parkhill J, Dougan G. 2009. Antibiotic treatment of
524 *Clostridium difficile* carrier mice triggers a supershedder state, spore-mediated transmission, and
525 severe disease in immunocompromised hosts. *Infection and Immunity* 77:3661–3669.
- 526 47. Lawley TD, Clare S, Walker AW, Stares MD, Connor TR, Raisen C, Goulding D, Rad R,
527 Schreiber F, Brandt C, Deakin LJ, Pickard DJ, Duncan SH, Flint HJ, Clark TG, Parkhill J, Dougan
528 G. 2012. Targeted restoration of the intestinal microbiota with a simple, defined bacteriotherapy
529 resolves relapsing *Clostridium difficile* disease in mice. *PLoS Pathogens* 8:e1002995.
- 530 48. Jump RLP, Polinkovsky A, Hurless K, Sitzlar B, Eckart K, Tomas M, Deshpande A, Nerandzic
531 MM, Donskey CJ. 2014. Metabolomics analysis identifies intestinal microbiota-derived biomarkers
532 of colonization resistance in clindamycin-treated mice. *PLoS ONE* 9:e101267.
- 533 49. Nagao-Kitamoto H, Leslie JL, Kitamoto S, Jin C, Thomsson KA, Gilliland MG, Kuffa P, Goto Y,
534 Jenq RR, Ishii C, Hirayama A, Seekatz AM, Martens EC, Eaton KA, Kao JY, Fukuda S, Higgins PDR,
535 Karlsson NG, Young VB, Kamada N. 2020. Interleukin-22-mediated host glycosylation prevents
536 *Clostridioides difficile* infection by modulating the metabolic activity of the gut microbiota. *Nature
537 Medicine* 26:608–617.
- 538 50. Battaglioli EJ, Hale VL, Chen J, Jeraldo P, Ruiz-Mojica C, Schmidt BA, Rekdal VM, Till LM, Huq
539 L, Smits SA, Moor WJ, Jones-Hall Y, Smyrk T, Khanna S, Pardi DS, Grover M, Patel R, Chia N,
540 Nelson H, Sonnenburg JL, Farrugia G, Kashyap PC. 2018. *Clostridioides difficile* uses amino acids
541 associated with gut microbial dysbiosis in a subset of patients with diarrhea. *Science Translational
542 Medicine* 10:eaam7019.
- 543 51. Robinson CD, Auchtung JM, Collins J, Britton RA. 2014. Epidemic *Clostridium difficile* strains
544 demonstrate increased competitive fitness compared to nonepidemic isolates. *Infection and
545 Immunity* 82:2815–2825.
- 546 52. Collins J, Auchtung JM, Schaefer L, Eaton KA, Britton RA. 2015. Humanized microbiota mice
547 as a model of recurrent *Clostridium difficile* disease. *Microbiome* 3.
- 548 53. Collins J, Robinson C, Danhof H, Knetsch CW, Leeuwen HC van, Lawley TD, Auchtung JM,

- 549 Britton RA. 2018. Dietary trehalose enhances virulence of epidemic *Clostridium difficile*. Nature
550 553:291–294.
- 551 54. Hryckowian AJ, Treuren WV, Smits SA, Davis NM, Gardner JO, Bouley DM, Sonnenburg JL.
552 2018. Microbiota-accessible carbohydrates suppress *Clostridium difficile* infection in a murine
553 model. *Nature Microbiology* 3:662–669.
- 554 55. Fouladi F, Glenny EM, Bulik-Sullivan EC, Tsilimigras MCB, Sioda M, Thomas SA, Wang Y, Djukic
555 Z, Tang Q, Tarantino LM, Bulik CM, Fodor AA, Carroll IM. 2020. Sequence variant analysis reveals
556 poor correlations in microbial taxonomic abundance between humans and mice after gnotobiotic
557 transfer. *The ISME Journal*.
- 558 56. Walter J, Armet AM, Finlay BB, Shanahan F. 2020. Establishing or exaggerating causality for
559 the gut microbiome: Lessons from human microbiota-associated rodents. *Cell* 180:221–232.
- 560 57. Rasmussen TS, Vries L de, Kot W, Hansen LH, Castro-Mejía JL, Vogensen FK, Hansen AK,
561 Nielsen DS. 2019. Mouse vendor influence on the bacterial and viral gut composition exceeds the
562 effect of diet. *Viruses* 11:435.
- 563 58. Mims TS, Abdallah QA, Watts S, White C, Han J, Willis KA, Pierre JF. 2020. Variability in
564 interkingdom gut microbiomes between different commercial vendors shapes fat gain in response
565 to diet. *The FASEB Journal* 34:1–1.
- 566 59. Stewart DB, Wright JR, Fowler M, McLimans CJ, Tokarev V, Amaniera I, Baker O, Wong H-T,
567 Brabec J, Drucker R, Lamendella R. 2019. Integrated meta-omics reveals a fungus-associated
568 bacteriome and distinct functional pathways in *Clostridioides difficile* infection. *mSphere* 4.
- 569 60. Ott SJ, Waetzig GH, Rehman A, Moltzau-Anderson J, Bharti R, Grasis JA, Cassidy L, Tholey A,
570 Fickenscher H, Seegert D, Rosenstiel P, Schreiber S. 2017. Efficacy of sterile fecal filtrate transfer
571 for treating patients with *Clostridium difficile* infection. *Gastroenterology* 152:799–811.e7.
- 572 61. Zuo T, Wong SH, Lam K, Lui R, Cheung K, Tang W, Ching JYL, Chan PKS, Chan MCW, Wu
573 JCY, Chan FKL, Yu J, Sung JJY, Ng SC. 2017. Bacteriophage transfer during faecal microbiota
574 transplantation in *Clostridium difficile* infection is associated with treatment outcome. *Gut*

- 575 gutjnl–2017–313952.
- 576 62. Zuo T, Wong SH, Cheung CP, Lam K, Lui R, Cheung K, Zhang F, Tang W, Ching JYL, Wu JCY,
577 Chan PKS, Sung JJY, Yu J, Chan FKL, Ng SC. 2018. Gut fungal dysbiosis correlates with reduced
578 efficacy of fecal microbiota transplantation in *Clostridium difficile* infection. Nature Communications
579 9.
- 580 63. Robinson JI, Weir WH, Crowley JR, Hink T, Reske KA, Kwon JH, Burnham C-AD, Dubberke
581 ER, Mucha PJ, Henderson JP. 2019. Metabolomic networks connect host-microbiome processes to
582 human *Clostridioides difficile* infections. Journal of Clinical Investigation 129:3792–3806.
- 583 64. Fletcher JR, Erwin S, Lanzas C, Theriot CM. 2018. Shifts in the gut metabolome and *Clostridium*
584 *difficile* transcriptome throughout colonization and infection in a mouse model. mSphere 3.
- 585 65. Xiao L, Feng Q, Liang S, Sonne SB, Xia Z, Qiu X, Li X, Long H, Zhang J, Zhang D, Liu C, Fang
586 Z, Chou J, Glanville J, Hao Q, Kotowska D, Colding C, Licht TR, Wu D, Yu J, Sung JJY, Liang Q, Li
587 J, Jia H, Lan Z, Tremaroli V, Dworzynski P, Nielsen HB, Bäckhed F, Doré J, Chatelier EL, Ehrlich
588 SD, Lin JC, Arumugam M, Wang J, Madsen L, Kristiansen K. 2015. A catalog of the mouse gut
589 metagenome. Nature Biotechnology 33:1103–1108.
- 590 66. Vital M, Rud T, Rath S, Pieper DH, Schlüter D. 2019. Diversity of bacteria exhibiting bile
591 acid-inducible 7alpha-dehydroxylation genes in the human gut. Computational and Structural
592 Biotechnology Journal 17:1016–1019.
- 593 67. Fransen F, Zagato E, Mazzini E, Fosso B, Manzari C, Aidy SE, Chiavelli A, D'Erchia AM,
594 Sethi MK, Pabst O, Marzano M, Moretti S, Romani L, Penna G, Pesole G, Rescigno M. 2015.
595 BALB/c and C57BL/6 mice differ in polyreactive IgA abundance, which impacts the generation of
596 antigen-specific IgA and microbiota diversity. Immunity 43:527–540.
- 597 68. Ivanov II, Atarashi K, Manel N, Brodie EL, Shima T, Karaoz U, Wei D, Goldfarb KC, Santee
598 CA, Lynch SV, Tanoue T, Imaoka A, Itoh K, Takeda K, Umesaki Y, Honda K, Littman DR. 2009.
599 Induction of intestinal th17 cells by segmented filamentous bacteria. Cell 139:485–498.
- 600 69. Azrad M, Hamo Z, Tkhawkho L, Peretz A. 2018. Elevated serum immunoglobulin a levels in

- 601 patients with *Clostridium difficile* infection are associated with mortality. *Pathogens and Disease* 76.
- 602 70. Saleh MM, Frisbee AL, Leslie JL, Buonomo EL, Cowardin CA, Ma JZ, Simpson ME, Scully KW,
603 Abhyankar MM, Petri WA. 2019. Colitis-induced th17 cells increase the risk for severe subsequent
604 *Clostridium difficile* infection. *Cell Host & Microbe* 25:756–765.e5.
- 605 71. Kozich JJ, Westcott SL, Baxter NT, Highlander SK, Schloss PD. 2013. Development of a
606 dual-index sequencing strategy and curation pipeline for analyzing amplicon sequence data on the
607 MiSeq illumina sequencing platform. *Applied and Environmental Microbiology* 79:5112–5120.
- 608 72. Sze MA, Schloss PD. 2019. The impact of DNA polymerase and number of rounds of
609 amplification in PCR on 16S rRNA gene sequence data. *mSphere* 4.
- 610 73. Schloss PD, Westcott SL, Ryabin T, Hall JR, Hartmann M, Hollister EB, Lesniewski RA,
611 Oakley BB, Parks DH, Robinson CJ, Sahl JW, Stres B, Thallinger GG, Horn DJV, Weber CF.
612 2009. Introducing mothur: Open-source, platform-independent, community-supported software
613 for describing and comparing microbial communities. *Applied and Environmental Microbiology*
614 75:7537–7541.
- 615 74. Quast C, Pruesse E, Yilmaz P, Gerken J, Schweer T, Yarza P, Peplies J, Glöckner FO. 2012.
616 The SILVA ribosomal RNA gene database project: Improved data processing and web-based tools.
617 *Nucleic Acids Research* 41:D590–D596.
- 618 75. Cole JR, Wang Q, Fish JA, Chai B, McGarrell DM, Sun Y, Brown CT, Porras-Alfaro A, Kuske CR,
619 Tiedje JM. 2013. Ribosomal database project: Data and tools for high throughput rRNA analysis.
620 *Nucleic Acids Research* 42:D633–D642.
- 621 76. Westcott SL, Schloss PD. 2017. OptiClust, an improved method for assigning amplicon-based
622 sequence data to operational taxonomic units. *mSphere* 2.
- 623 77. Oksanen J, Blanchet FG, Friendly M, Kindt R, Legendre P, McGlinn D, Minchin PR, O'Hara RB,
624 Simpson GL, Solymos P, Stevens MHH, Szoecs E, Wagner H. 2018. Vegan: Community ecology

625 package.

626 78. R Core Team. 2018. R: A language and environment for statistical computing. R Foundation for
627 Statistical Computing, Vienna, Austria.

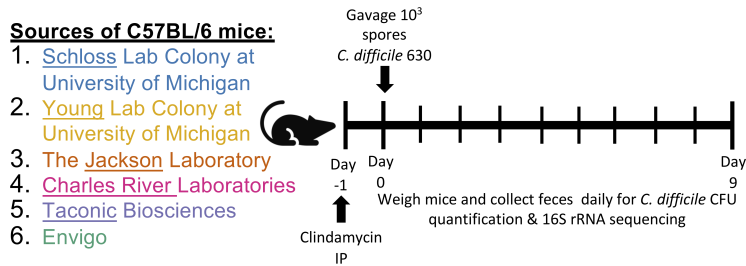
628 79. Kuhn M. 2008. Building predictive models inRUsing thecaretPackage. Journal of Statistical
629 Software 28.

630 80. Topçuoğlu BD, Lesniak NA, Ruffin MT, Wiens J, Schloss PD. 2020. A framework for effective
631 application of machine learning to microbiome-based classification problems. mBio 11.

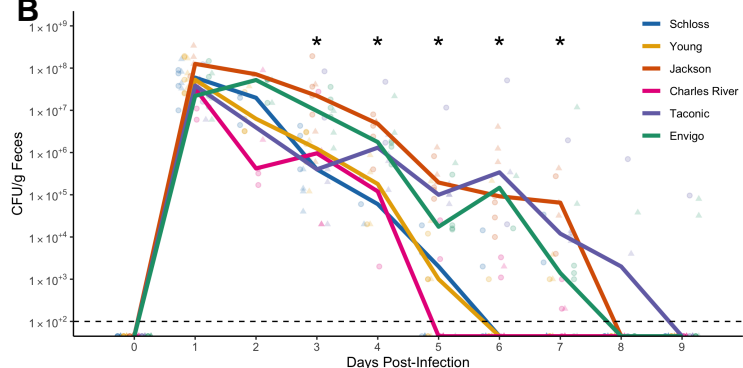
632 81. Wickham H, Averick M, Bryan J, Chang W, McGowan LD, François R, Grolemund G, Hayes
633 A, Henry L, Hester J, Kuhn M, Pedersen TL, Miller E, Bache SM, Müller K, Ooms J, Robinson D,
634 Seidel DP, Spinu V, Takahashi K, Vaughan D, Wilke C, Woo K, Yutani H. 2019. Welcome to the
635 tidyverse. Journal of Open Source Software 4:1686.

636 **Figures**

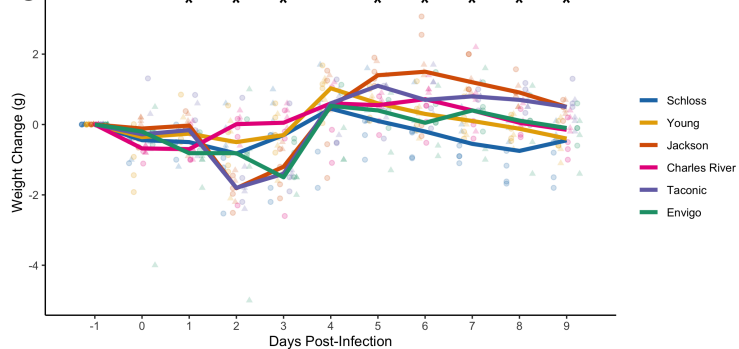
A



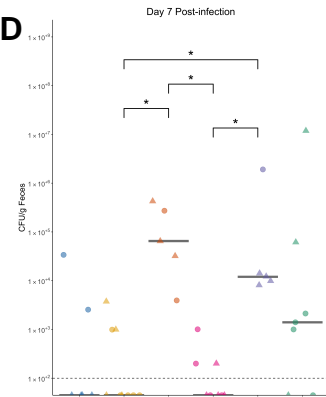
B



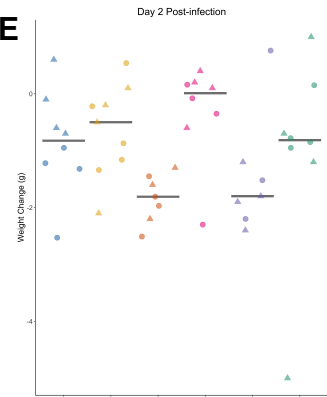
C



D



E

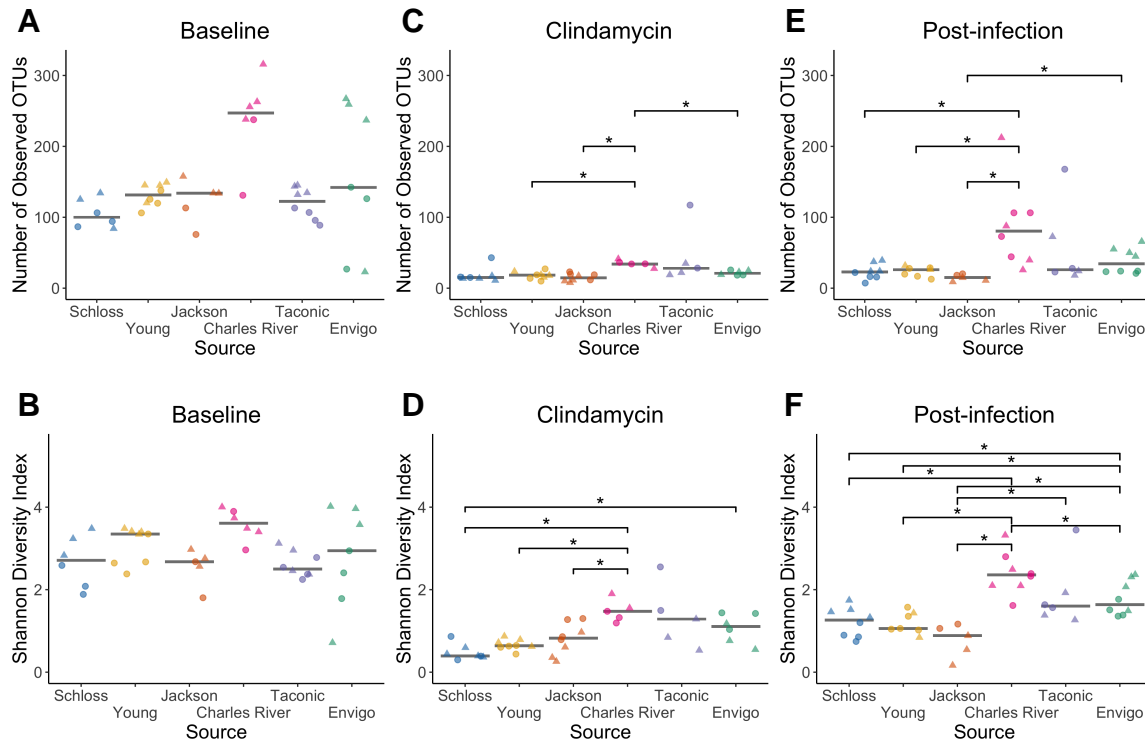


637

Figure 1. Clindamycin is sufficient

to promote *C. difficile* colonization in all mice, but clearance time varies across sources of

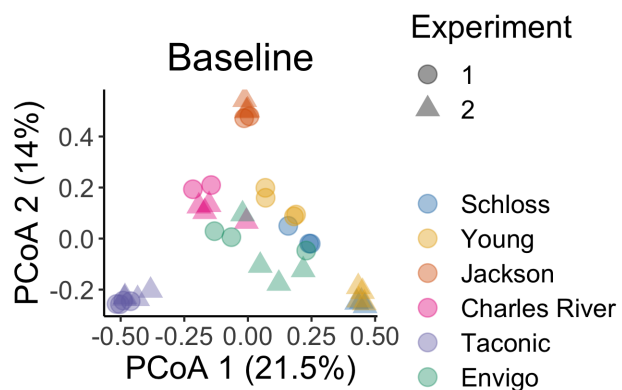
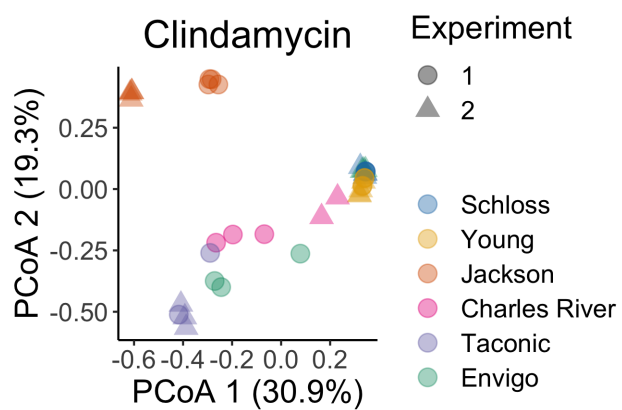
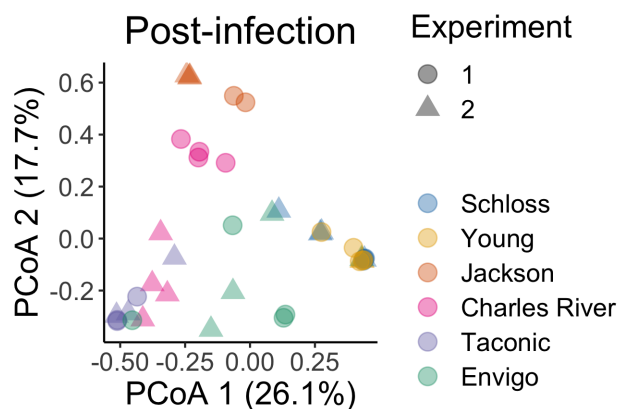
639 **C57BL/6 mice.** A. Setup of the experimental timeline. Mice for the experiments were obtained
640 from 6 different sources: the Schloss ($N = 8$) and Young lab ($N = 9$) colonies at the University of
641 Michigan, the Jackson Laboratory ($N = 8$), Charles River Laboratory ($N = 8$), Taconic Biosciences
642 ($N = 8$), and Envigo ($N = 8$). All mice were administered 10 mg/kg clindamycin intraperitoneally
643 (IP) 1 day before challenge with *C. difficile* 630 spores on day 0. Mice were weighed and feces
644 was collected daily through the end of the experiment (9 days post-infection). Note: 3 mice died
645 during course of experiment. 1 Taconic mouse prior to infection and 1 Jackson and 1 Envigo mouse
646 between 1- and 3-days post-infection. B. *C. difficile* CFU/gram stool measured over time ($N =$
647 20-49 mice per timepoint) via serial dilutions. The black line represents the limit of detection for
648 the first serial dilution. CFU quantification data was not available for each mouse due to early
649 deaths, stool sampling difficulties, and not plating all of the serial dilutions. C. Mouse weight change
650 measured in grams over time ($N = 45-49$ mice per timepoint), all mice were normalized to the
651 weight recorded 1 day before infection. For B-C: timepoints where differences across sources
652 of mice were statistically significant by Kruskal-Wallis test with Benjamini-Hochberg correction
653 for testing across multiple days (Table S1 and Table S2) are reflected by the asterisk(s) above
654 each timepoint (*, $P < 0.05$). Lines represent the median for each source and circles represent
655 individual mice from experiment 1 while triangles represent mice from experiment 2. D. *C. difficile*
656 CFU/gram stool on day 7 post-infection across sources of mice with asterisks for pairwise Wilcoxon
657 comparisons with Benjamini-Hochberg correction where $P < 0.05$. E. Mouse weight change 2 days
658 post-infection across sources of mice, no pairwise Wilcoxon comparisons were significant after
659 Benjamini-Hochberg correction. For D-E. Circles represent experiment 1 mice, triangles represent
660 experiment 2 mice and gray lines indicate the median values for each group.



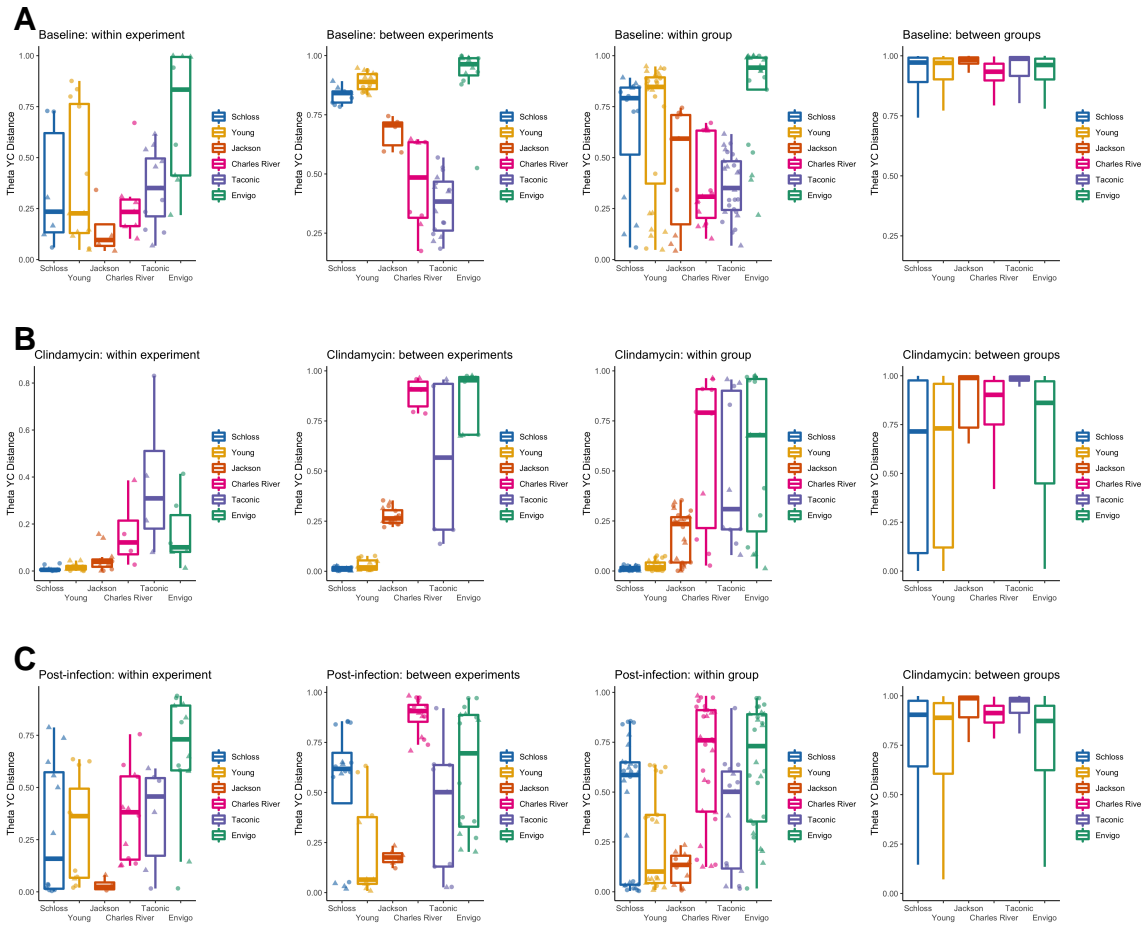
Figure

661

662 **2. Differences in microbial richness and diversity across mouse colony sources emerge**
 663 **after clindamycin treatment and infection.** A-F. Number of observed OTUs and Shannon
 664 diversity index values at baseline: day -1 (A-B), after clindamycin: day 0 (C-D) and post-infection:
 665 day 1 (E-F) timepoints of the experiment. Data were analyzed by Kruskal-Wallis test with
 666 Benjamini-Hochberg correction for testing each day of the experiment and the adjusted P value
 667 was < 0.05 for all panels except for B (Table S3). Significant P values from the pairwise Wilcoxon
 668 comparisons between sources with Benjamini-Hochberg correction are shown (Table S4). For
 669 A-F: circles represent experiment 1 mice, while triangles represent experiment 2 mice with each
 670 symbol representing the value for a stool sample from an individual mouse. Gray lines represent
 671 the median values for each source of mice.

A**B****C****Figure 3. Mouse colony**

673 **source is the variable that explains most of the variation observed in the baseline,**
674 **post-clindamycin, and post-infection bacterial communities.** A-C. Principal Coordinates
675 Analysis of Theta YC distances from stools collected at baseline (A), post-clindamycin (B), and
676 post-infection (C) timepoints of the experiment. Each symbol represents a stool sample from
677 an individual mouse, with circles representing experiment 1 mice and triangles representing
678 experiment 2 mice. PERMANOVA analysis demonstrated that source and the interaction between
679 source and cage explained most of the variation observed in the baseline (combined $R^2 = 0.90$),
680 post-clindamycin (combined $R^2 = 0.99$), and post-infection (combined $R^2 = 0.88$) communities (all
681 $P = 0.0001$, see Table S6).

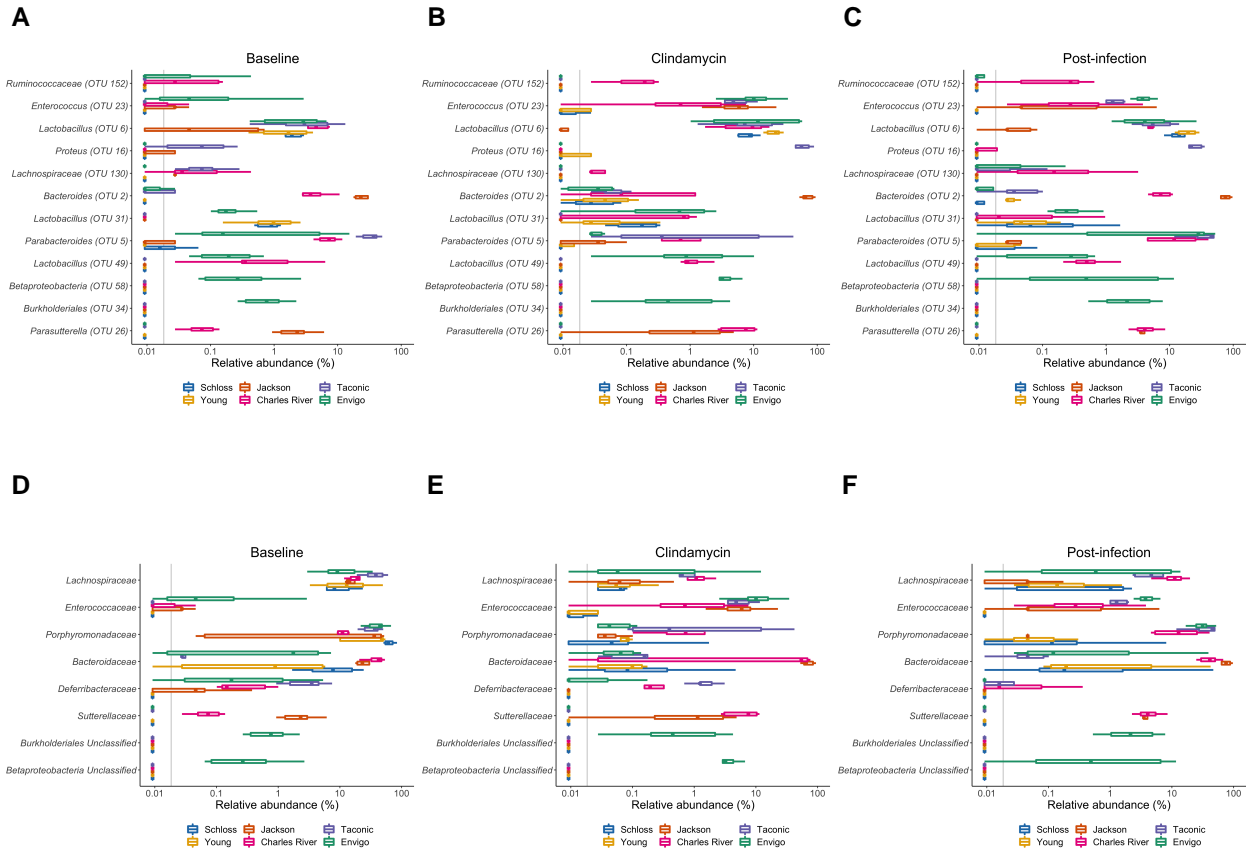


Figure

682

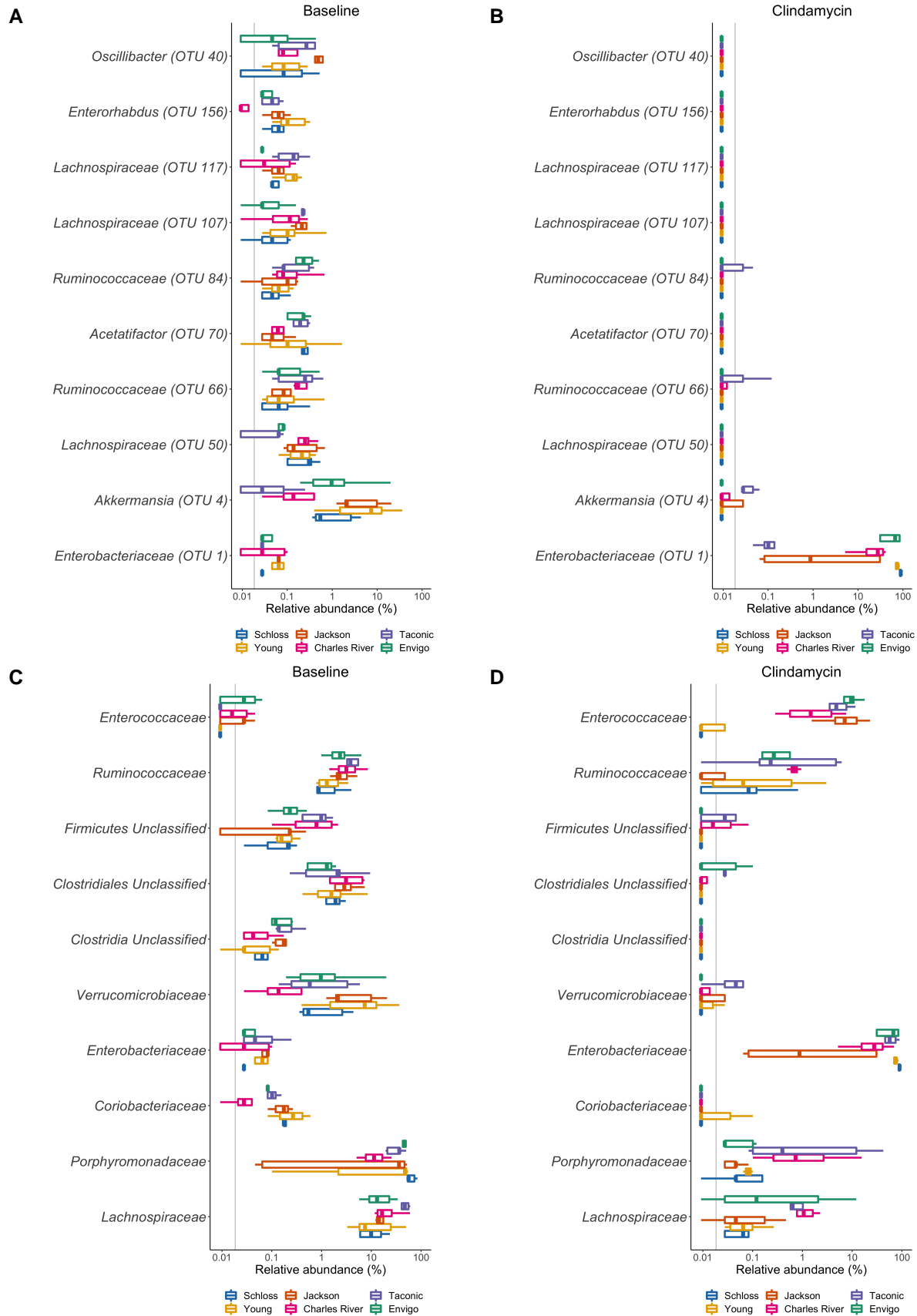
683 **4. High inter-group variation across mouse sources is diminished by clindamycin treatment**

684 A-C. Boxplots of the Theta YC distances of the 6 sources of mice relative to mice within the same
 685 source and experiment, mice within the same source and between experiments, mice within the
 686 same source, and mice from other groups at the baseline (A), after clindamycin treatment (B),
 687 and post-infection (C) timepoints. For comparisons within mice from the same source, symbols
 688 represent individual mouse samples: circles for experiment 1 and triangles for experiment 2.

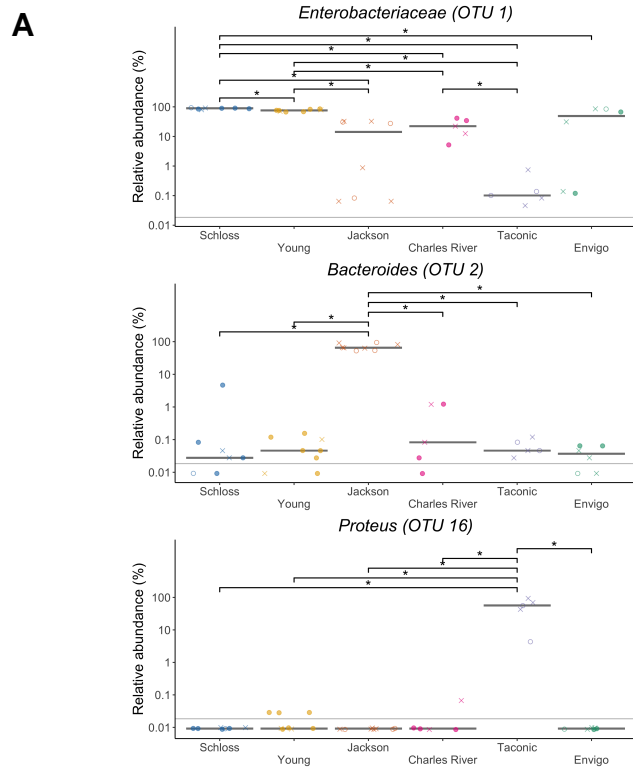


689

690 **Figure 5. A subset of bacteria consistently vary across mouse colony sources despite**
 691 **clindamycin perturbation and *C. difficile* challenge.** A-C. Boxplots of the relative abundances
 692 for the 12 OTUs that consistently varied across sources of mice at the baseline (A), post-clindamycin
 693 (B), and post-infection (C) timepoints of the experiment. D-F. Boxplots of the relative abundances for
 694 the 8 families that consistently varied across sources of mice at the baseline (D), post-clindamycin
 695 (E), and post-infection (F) timepoints of the experiment. For each timepoint bacteria with differential
 696 relative abundances across sources of mice were identified by Kruskal-Wallis test at the family and
 697 OTU level with Benjamini-Hochberg correction for testing all identified taxa at the respective level
 698 (Table S8-9). The grey vertical line indicates the limit of detection for A-F.



700 **Figure 6. Clindamycin treatment has the same effects on a subset of taxa regardless of**
701 **colony source.** A-B. Boxplots of the top 10 most significant (adjusted *P* value < 0.05) OTUs with
702 relative abundances that changed post clindamycin treatment. C-D. Boxplots of the top 10 most
703 significant families with relative abundances that changed post clindamycin treatment. Data were
704 analyzed by Wilcoxon signed rank test limited to mice that had paired sequence data for day -1
705 and 0 (*N* = 31). Tests were performed at the OTU and family levels with Benjamini-Hochberg
706 correction for testing all identified OTUs and families. See Table S10-11 for complete list of OTUs
707 and families significantly impacted by clindamycin treatment. The grey vertical line indicates the
708 limit of detection for A-D.



B

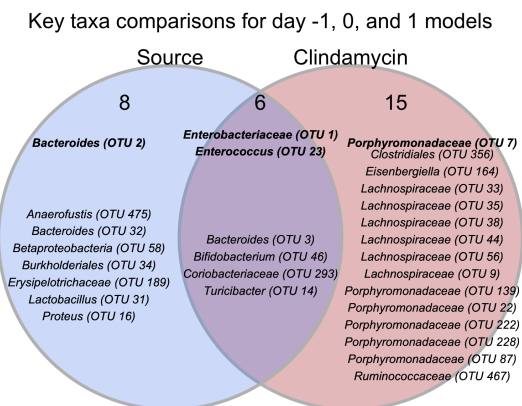


Figure 7. Key OTUs that influence

709

710 **whether mice cleared *C. difficile* by day 7.** A. Baseline relative abundance data for 3 of the
 711 OTUs from the classification model based on day 0 OTU relative abundances that significantly
 712 varied across sources of mice and had high relative abundances. Symbols represent the relative

abundance data for an individual mouse, circles represent mice that cleared *C. difficile* by day 7, X-shapes represent mice that were still colonized with *C. difficile*, and open circles represent mice that did not have *C. difficile* CFU counts for day 7 post-infection. Gray lines indicate the median relative abundances for each source. Asterisks are shown for pairwise Wilcoxon comparisons with Benjamini-Hochberg correction where $P < 0.05$. B. Venn diagram that combines Fig. S4 summaries of OTUs that were important to the day -1, 0, and 1 classification models (Table S14) and either overlapped with taxa that varied across vendors at the same timepoint, were impacted by clindamycin treatment, or both. See Fig. S4 for separate comparisons of taxa from the day -1, 0, and 1 classification models. Bold OTUs signify OTUs that were important to more than 1 classification model.

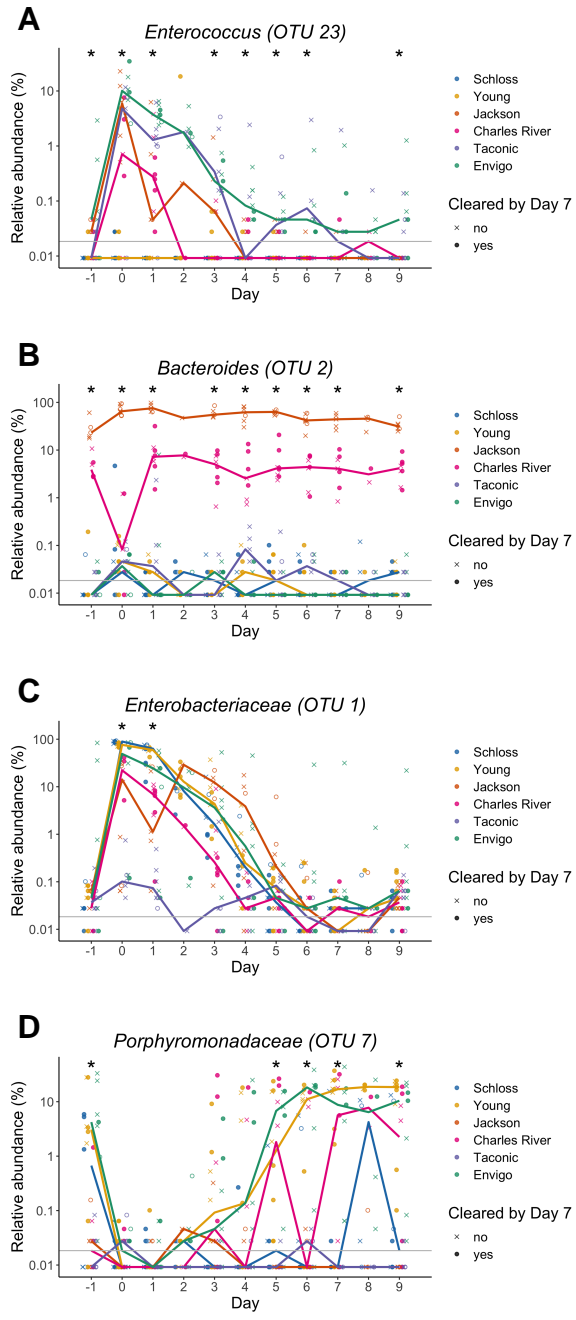


Figure 8: Key OTUs vary across sources

723

724 **throughout the experiment.** A-C. Relative abundances of bold OTUs from Fig. 7A that

725 were important for at least two classification models are shown over time. A. *Enterococcus*

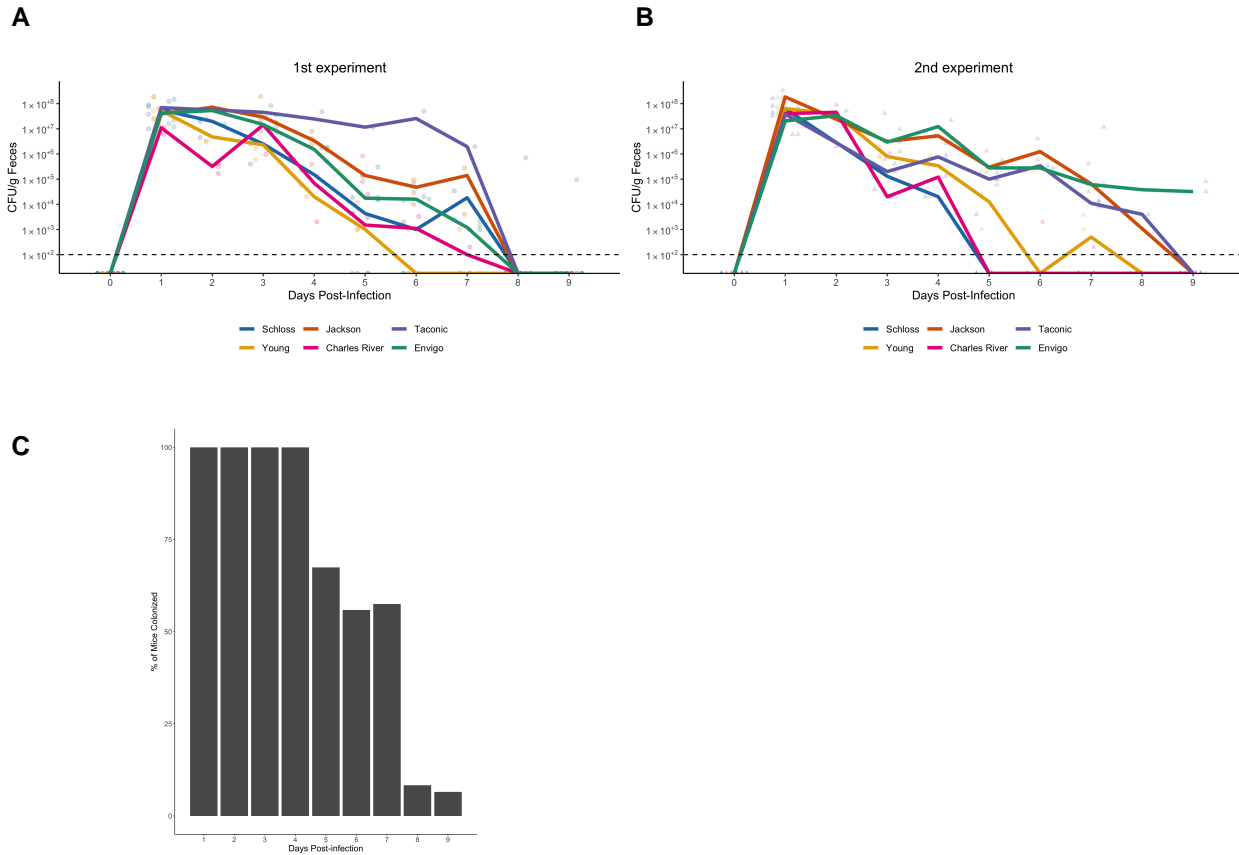
726 (OTU 23), which significantly varied across sources and was impacted by clindamycin

727 treatment. B. *Bacteroides* (OTU 2), which varied across sources throughout the experiment. C.

728 *Enterobacteriaceae* (OTU 1) and *Porphyromonadaceae* (OTU 7) were significantly impacted

729 by clindamycin treatment and examining relative abundance dynamics over the course of the

730 experiment indicated timepoints where relative abundances also significantly varied across sources
731 of mice. Symbols represent the relative abundance data for an individual mouse, circles represent
732 mice that cleared *C. difficile* by day 7, X-shapes represent mice that were still colonized with
733 *C. difficile*, and open circles represent mice that did not have *C. difficile* CFU counts for day 7
734 post-infection. Colored lines indicate the median relative abundances for each source. The gray
735 horizontal line represents the limit of detection. Timepoints where differences across sources of
736 mice were statistically significant by Kruskal-Wallis test with Benjamini-Hochberg correction for
737 testing across multiple days (Table S16) are identified by the asterisk(s) above each timepoint (*, P
738 < 0.05).



739

740 **Figure S1. *C. difficile* CFU variation across vendors varies slightly across the 2**
 741 **experiments.** A-B. *C. difficile* CFU/gram of stool quantification over time for experiment 1
 742 (A) and 2 (B). Experiments were conducted approximately 3 months apart. Lines represent the
 743 median CFU for each source, symbols represent individual mice and the black line represents the
 744 limit of detection. C. Percent of mice that were colonized with *C. difficile* over the course of the
 745 experiment. Each day the percent is calculated based on the mice where *C. difficile* CFU was
 746 quantified for that particular day. Total N for each day: day 1 (N = 42), day 2 (N = 20), day 3 (N =
 747 39), day 4 (N = 29), day 5 (N = 43), day 6 (N = 34), day 7 (N = 40), day 8 (N = 36), and day 9 (N =
 748 46).

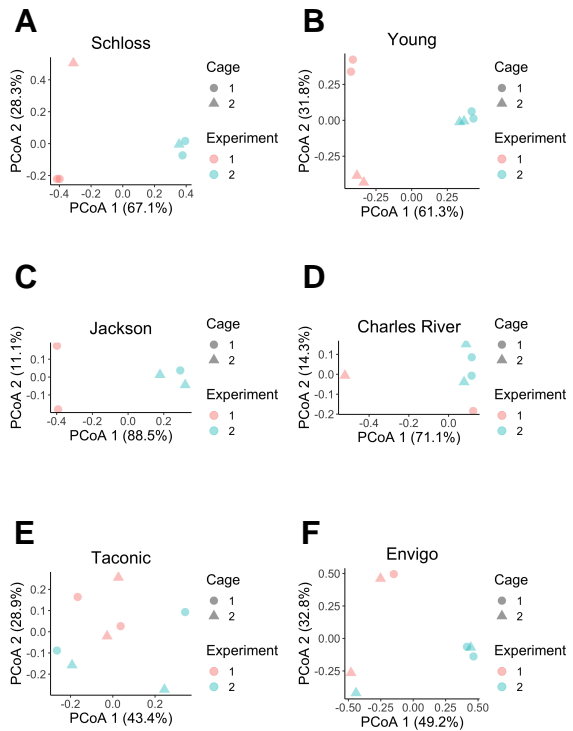
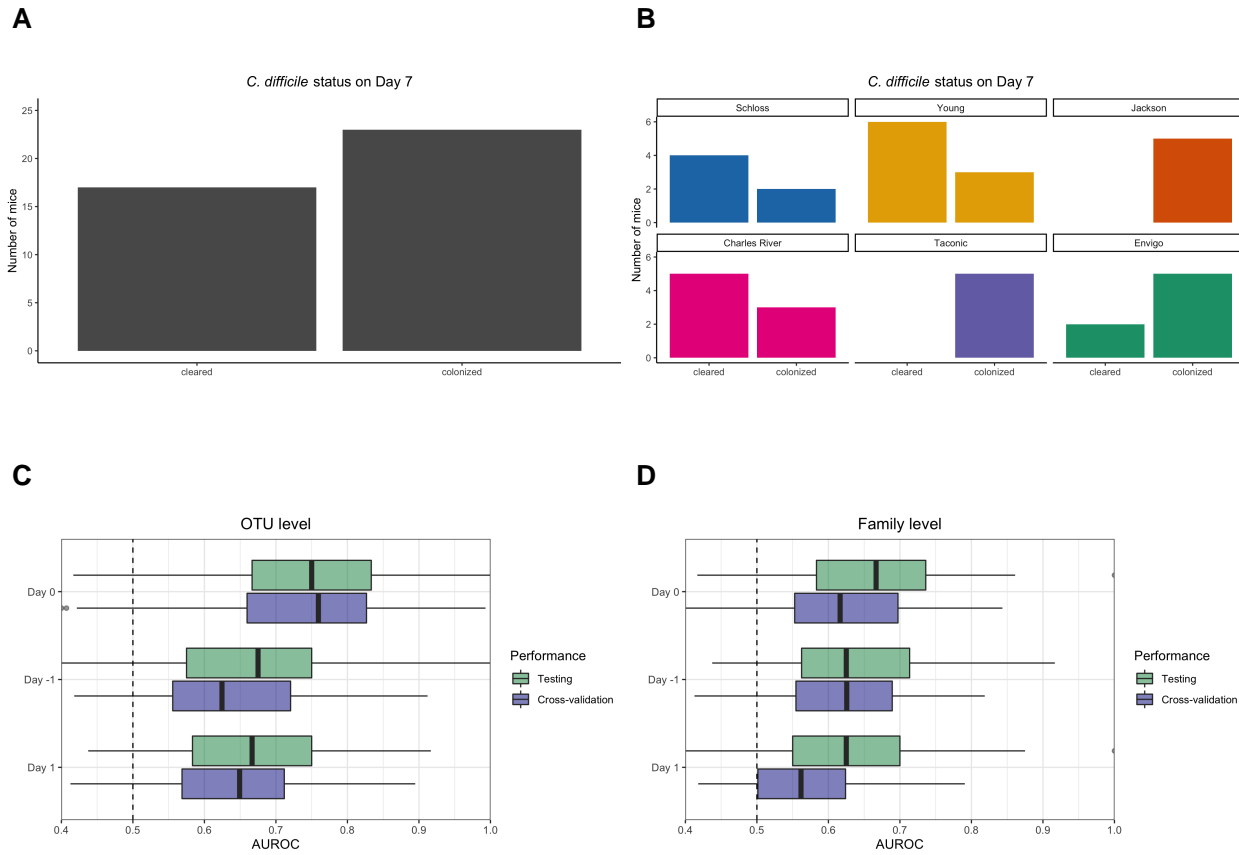


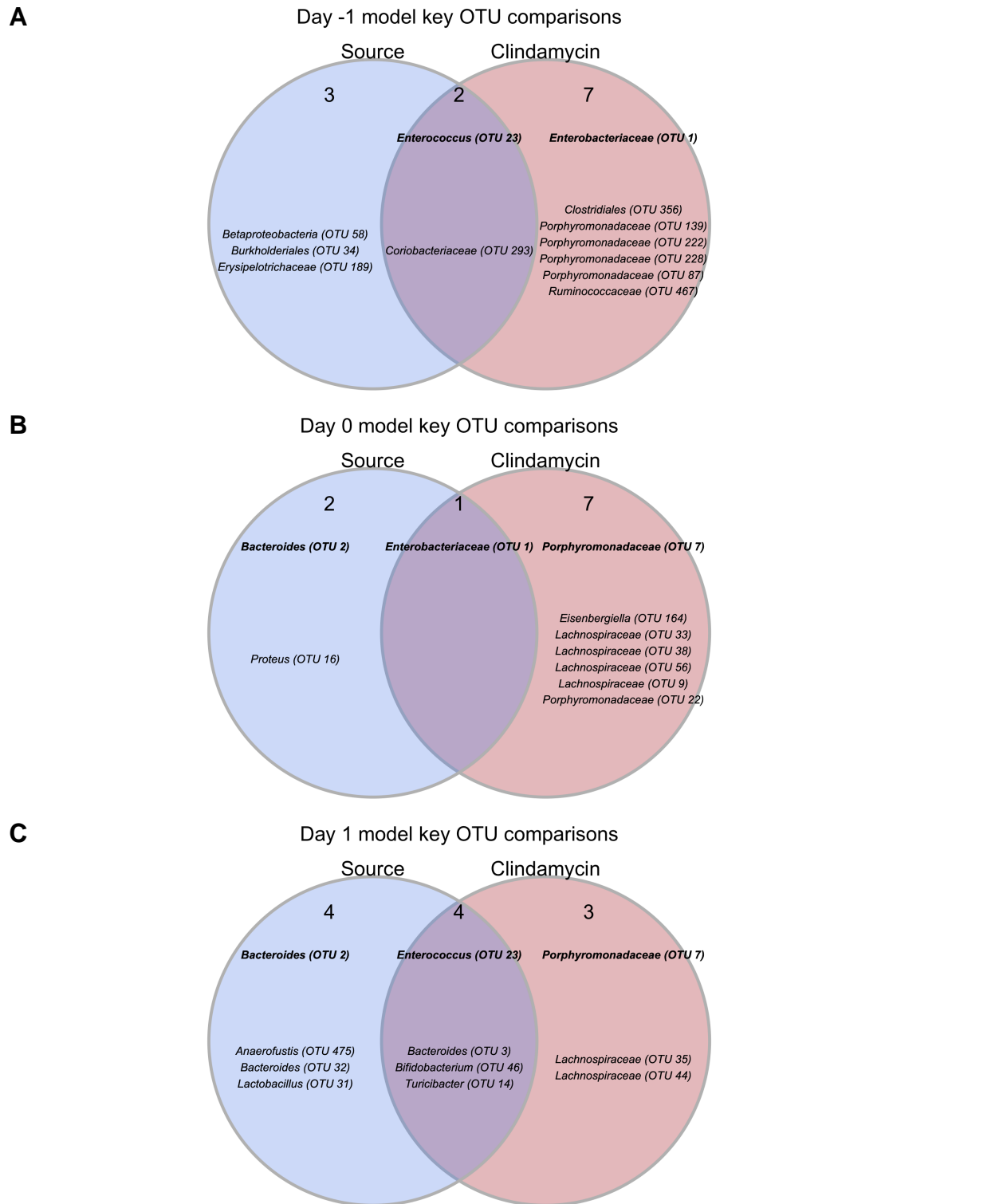
Figure S2. Only bacterial communities from

749 **University of Michigan mice significantly vary between experiments.** A-F. PCoA of Theta YC
 750 distances for the baseline fecal bacterial communities within each source of mice. Each symbol
 751 represents a stool sample from an individual mouse with color corresponding to experiment and
 752 shape representing cage mates. PERMANOVA was performed within each group to examine the
 753 contributions of experiment and cage to observed variation. Experiment number and cage only
 754 significantly explained observed variation for mice from the Schloss (combined $R^2 = 0.99$; $P \leq$
 755 0.033) and Young (combined $R^2 = 0.95$; $P \leq 0.027$) lab colonies (Table S7).



757

758 **Figure S3. Bacterial community composition before, after clindamycin perturbation, and**
 759 **post-infection can predict *C. difficile* colonization status 7 days post-challenge.** A. Bar
 760 graph visualizations of overall day 7 *C. difficile* colonization status that were used as classification
 761 outcomes to build logistic regression models. Mice were classified as colonized or cleared
 762 (not detectable at the limit of detection of 100 CFU) based on CFU g/stool data from 7 days
 763 post-infection. B. *C. difficile* CFU status on Day 7 within each mouse colony source. N = 5-9
 764 mice per group. C-D. L2-regularized logistic regression classification model AUROCs to predict *C.*
765 difficile CFU on D7 (Fig. 1D, Fig. S3) based on the community relative abundances at baseline
 766 (day -1), post-clindamycin (day 0), and post-infection (day 1) at either the OTU (C) or family (D)
 767 level. All models performed better than random chance (AUROC = 0.5), see (all $P \leq 5e-15$; Table
 768 S12) and the model built with post-clindamycin treated bacterial OTU relative abundances had the
 769 best performance ($P_{FDR} \leq 3.9e-10$ for pairwise comparisons; Table S13). A List of the 20 taxa that
 770 were ranked as most important to each model are listed in Table S14-15.



Figure

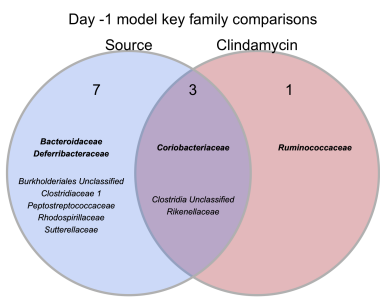
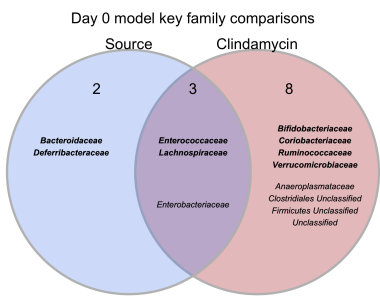
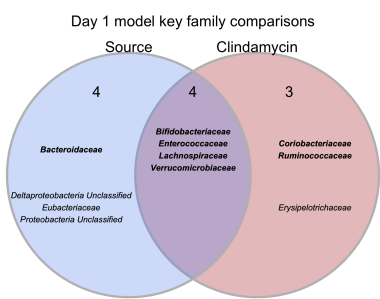
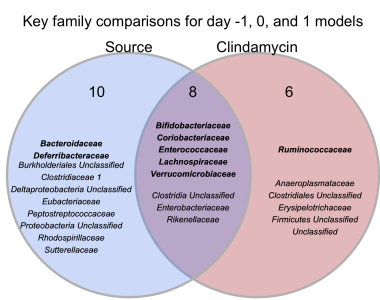
771

772 **S4. Key OTUs from classification models based on baseline, post-clindamycin treatment,**

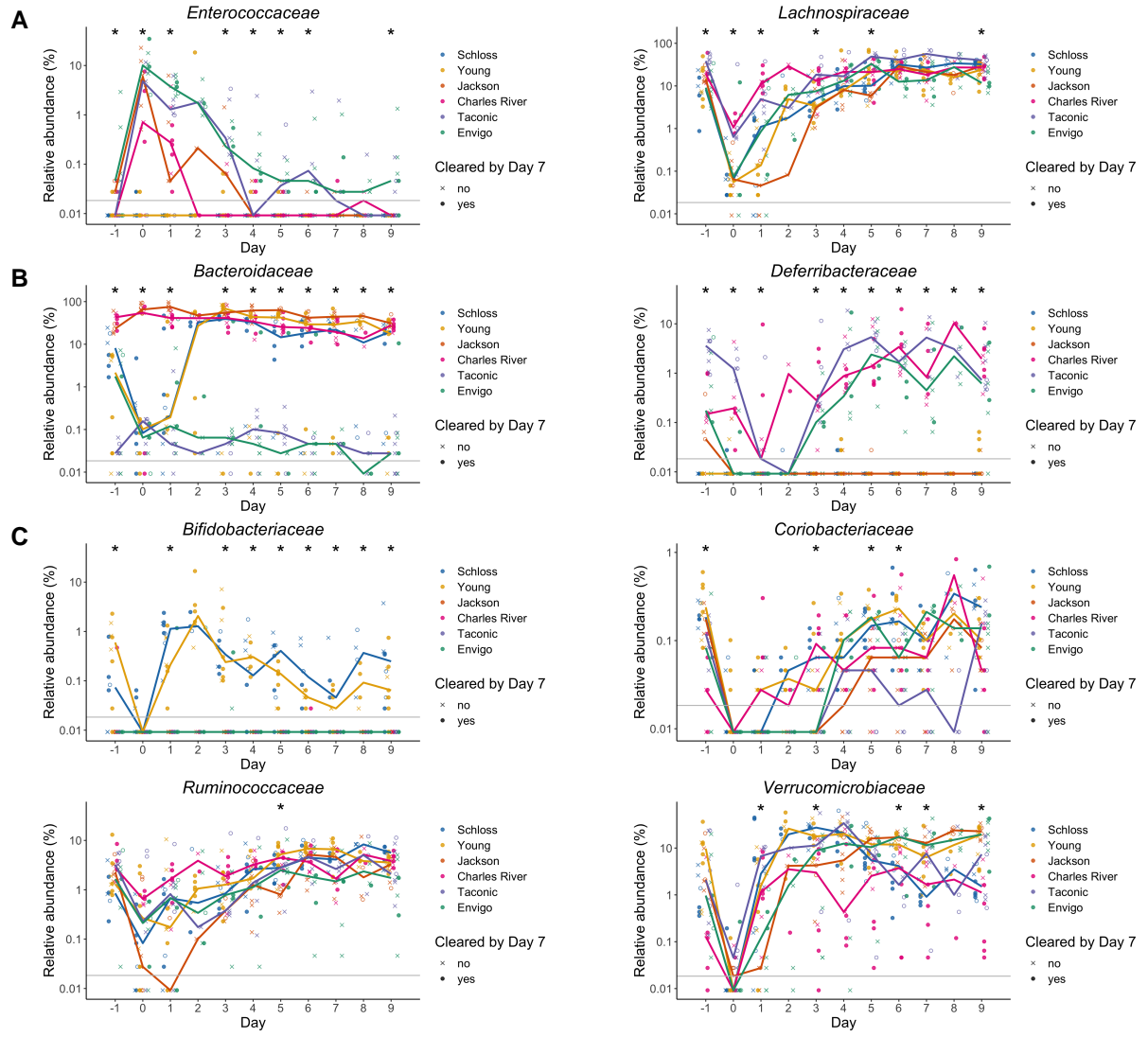
773 **or post-infection community data vary by mouse colony source, clindamycin treatment, or**

774 **both.** A-C. Venn diagrams of top 20 important OTUs from baseline (A), post-clindamycin treatment

⁷⁷⁵ (B), and post-infection (C) classification models (Table S14) that overlapped with OTUs that varied
⁷⁷⁶ across vendors at baseline, were impacted by clindamycin treatment, or both. Bold OTUs signify
⁷⁷⁷ OTUs that were important to more than 1 classification model.

A**B****C****D****Figure S5. Key families from classification models**

779 **based on baseline, post-clindamycin treatment, or post-infection community data vary by**
780 **mouse colony source, clindamycin treatment, or both.** A-C. Venn diagrams of top 20 important
781 families from baseline (A), post-clindamycin treatment (B), and post-infection (C) classification
782 models (Table S15) that overlapped with families that varied across vendors after clindamycin, were
783 impacted by clindamycin treatment, or both. D. Venn diagrams that combines A-C summaries of
784 families that were important to the day -1, 0, and 1 classification models (Table S15) and either
785 overlapped with families that varied across vendors at the same timepoint, were impacted by
786 clindamycin treatment, or both. Bold families signify families that were important to more than 1
787 classification model.



788

789 **Figure S6. Key families vary across sources throughout experiment.** Relative abundances of
 790 bold families from Fig. S5D that were important for at least two classification models are shown
 791 over time. A. *Enterococcaceae* and *Lachnospiraceae*, which significantly varied across sources
 792 and were impacted by clindamycin treatment. B. *Bacteroidaceae* and *Deferrribacteraceae*, which
 793 varied across sources throughout the experiment. C. *Bifidobacteriaceae*, *Coriobacteriaceae*,
 794 *Ruminococcaceae*, and *Verrucomicrobiaceae* were significantly impacted by clindamycin treatment.
 795 Examining the relative abundance dynamics throughout the experiment, identified timepoints
 796 where relative abundances also significantly varied across sources of mice. Symbols represent the
 797 relative abundance data for an individual mouse, circles represent mice that cleared *C. difficile* by
 798 day 7, X-shapes represent mice that were still colonized with *C. difficile*, and open circles represent

799 mice that did not have *C. difficile* CFU counts for day 7 post-infection. Colored lines indicate the
800 median relative abundances for each source. The gray horizontal line represents the limit of
801 detection. Timepoints where differences across sources of mice were statistically significant by
802 Kruskal-Wallis test with Benjamini-Hochberg correction for testing across multiple days (Table S17)
803 are identified by the asterisk(s) above each timepoint (*, P < 0.05).

804 **Supplementary Tables and Movie**

805 All supplemental material is available at: https://github.com/SchlossLab/Tomkovich_vendor_difs_XXXX_2020.

807 **Movie S1. Large shifts in bacterial community structure occurred after clindamycin and *C.***
808 ***difficile* infection.** PCoA of Theta YC distances animated from 0 through 9 days post-infection.
809 PERMANOVA analysis indicated colony source was the variable that explained the most observed
810 variation across fecal communities (source $R^2 = 0.35$, $P = 0.0001$) followed by interactions between
811 cage and day of the experiment. Transparency of the circle corresponds to the day of the experiment,
812 each circle represents a sample from an individual mouse at a specific timepoint. See Table S5
813 for PERMANOVA results). Circles represent mice from experiment 1 and triangles represent mice
814 from expeirment 2.

815 **Table S1. *C. difficile* CFU statistical results.**

816 **Table S2. Mouse weight change statistical results.**

817 **Table S3. Diversity metrics Kruskal-Wallis statistical results.**

818 **Table S4. Diversity metrics pairwise Wilcoxon statistical results.**

819 **Table S5. PERMANOVA results for all mice, all timepoints.**

820 **Table S6. PERMANOVA results for all mice, all timepoints.**

821 **Table S7. PERMANOVA results of baseline communities within each source.**

822 **Table S8. OTUs with relative abudances that significantly vary across sources at baseline,**
823 **post-clindamycin, or post-infection timepoints.**

824 **Table S9. Families with relative abudances that significantly vary across sources at**
825 **baseline, post-clindamycin, or post-infection timepoints.**

826 **Table S10. OTUs with relative abudances that significantly changed after clindamycin**
827 **treatment.**

828 **Table S11.** Families with relative abundances that significantly changed after clindamycin
829 treatment. **Table S12.** Statistical results of L2-regularized logistic regression model
830 performances compared to random chance.

831 **Table S13.** Pairwise Wilcoxon results of comparing all 6 L2-regularized logistic regression
832 model performances.

833 **Table S14.** Top 20 most important OTUs for each of the 3 L2-regularized logistic regression
834 models based on OTU relative abundance data.

835 **Table S15.** Top 20 most important families for each of the 3 L2-regularized logistic
836 regression models based on OTU relative abundance data.

837 **Table S16.** OTUs with relative abundances that significantly varied across sources of mice
838 on at least 1 day of the experiment.

839 **Table S17.** Families with relative abundances that significantly varied across sources of mice
840 on at least 1 day of the experiment.